

Spectroscopic investigation of old planetaries

IV. Model atmosphere analysis

R. Napiwotzki *

Dr. Remeis-Sternwarte, Sternwartstr. 7, D-96049 Bamberg, Germany

Received date; accepted date

Abstract. The results of a NLTE model atmosphere analysis of 27 hydrogen-rich central stars of old planetary nebulae (PN) are reported. These stars were selected from a previous paper in this series, where we gave classifications for a total of 38 central stars. Most of the analyzed central stars fill a previously reported gap in the hydrogen-rich evolutionary sequence. Our observations imply the existence of two separated spectral evolutionary sequences for hydrogen-rich and -poor central stars/white dwarfs. This is in line with theoretical evolutionary calculations, which predict that most post-AGB stars reach the white dwarf domain with a thick hydrogen envelope of $\approx 10^{-4} M_{\odot}$.

We determine stellar masses from the comparison with evolutionary tracks and derive a mass distribution for the hydrogen-rich central stars of old PNe. The peak mass and the general shape of the distribution is in agreement with recent determinations of the white dwarf mass distribution.

The properties of most analyzed stars are well explained by standard post-AGB evolution. However, for eight stars of the sample other scenarios have to be invoked. The properties of three of them are probably best explained by born again post-AGB evolution. Two of these are hybrid CSPN (hydrogen-rich PG 1159 stars), but surprisingly the third star doesn't show any signs of chemical enrichment in its atmosphere. The parameters of five stars are not in accordance with post-AGB evolution. We discuss alternative scenarios such as the stripping of the hydrogen-rich envelope by a companion during the first red giant phase or the formation of a common envelope with a possible merging of both components. Two stars (HDW 4 and HaWe 5) remain mysterious after all. They resemble ordinary hot DA white dwarfs, but due to very large evolutionary ages the presence of a PN cannot be

explained. We speculate that the nebulae may be shells produced by ancient nova outbursts.

A wide spread of helium abundances is observed in the photospheres of central stars of old PNe. It is shown that a good correlation between helium abundances and luminosity is present. It is inferred that when the stars' luminosities fall below $L \approx 300L_{\odot}$ depletion starts and the helium abundance steadily decreases with decreasing luminosity. The existence of this correlation is in qualitative agreement with recent theoretical calculations of gravitational settling in the presence of a stellar wind.

Key words: stars: abundances — planetary nebulae: general — white dwarfs — stars: fundamental parameters

1. Introduction

Central stars of planetary nebulae (PN) are the immediate precursors of white dwarfs. Most stars enter the white dwarf cooling sequence through this evolutionary channel (Drilling & Schönberner 1985). After the maximum effective temperature is reached (100,000 K and more) the nuclear burning ceases, the surrounding nebula disperses, and the central star stage ends. Thus the nuclei of old PNe mark the transition to the white dwarfs. During this stage the onset of gravitational settling, which causes the chemical purity of many white dwarf atmospheres, can be observed.

Central stars of old PNe play a crucial role in our understanding of the formation of the two distinct sequences of central stars of planetary nebulae (CSPN) and white dwarfs: the hydrogen-rich and the hydrogen-deficient (helium- and carbon-rich) one. For the hydrogen-deficient CSPN there exists a continuous sequence from the luminous central stars (Wolf-Rayet stars of spectral type [WC]) to the low luminosity DO white dwarfs via the PG 1159 stars, hot pre-white dwarfs with typical temperatures of 100000 K. Méndez (1991) presented a compilation of spectral types for (mostly luminous) CSPN and found a fraction of about 1/3 hydrogen-deficient objects. Liebert (1986) reported a ratio of H-poor to H-rich stars

Send offprint requests to: Ralf Napiwotzki
(napiwotzki@sternwarte.uni-erlangen.de)

* Visiting astronomer, German-Spanish Astronomical Center, Calar Alto, Spain, operated by the Max-Planck-Institut für Astronomie, Heidelberg, jointly with the Spanish National Commission for Astronomy

of 1:(7±3) for the hot white dwarfs (spectral types DO and DA resp.) in the Palomar-Green survey (Green et al. 1986), but noted a lack of very hot DA white dwarfs (the counterparts of the PG 1159 stars). Holberg (1987) selected a sample of the apparently hottest DA/DAO white dwarfs from the PG survey and concluded that none of them appear to have a temperature in excess of 80000 K, with T_{eff} typically in the range 60000 K to 70000 K. However, detailed analyses of these stars were not presented.

Fontaine & Wesemael (1987) discussed this seeming lack of very hot H-rich white dwarfs and proposed that all CSPN finally lose their hydrogen-rich surface layer and evolve through one channel: the PG 1159/DO stars. After the stars have become white dwarfs gravitational settling causes small traces of hydrogen, hidden in the helium layer, to float up and form a very thin H-layer. This scenario is in contradiction to theoretical calculations (e.g. Schönberner 1981, 1983; Vassiliadis & Wood 1994; Blöcker 1995), which predict a “thick” H-layer of $\approx 10^{-4} M_{\odot}$, but could nicely explain many properties of white dwarfs known at that time (EUV/X-ray observations, the DB gap, pulsational properties of ZZ Ceti stars). Due to improved observations and increased theoretical knowledge the interpretation has changed during the last years and it is now generally accepted that the vast majority of DA white dwarfs possess a thick H-layer (cf. the recent review of Fontaine & Wesemael 1997). However, the interpretation of many observational results is not completely unambiguous. Vennes et al. (1997), e.g., analyzed a sample of EUV selected DA white dwarfs and compared their results with cooling tracks calculated with thick and with very thin layers. They found better agreement with the latter tracks and interpreted this result as evidence of a very thin hydrogen layer of most DA white dwarfs (but see discussion in Napiwotzki et al. 1999).

The Fontaine & Wesemael (1987) scenario makes one prediction concerning the stars just entering the white dwarf cooling sequence: the vast majority of them should be hydrogen-poor PG 1159 stars or DO white dwarfs. Although a small number of hydrogen-rich stars in this transition region don't contradict the very thin layer scenario (see discussion in Fontaine & Wesemael 1997), the hydrogen-poor ones should be the dominant species. The transition between CSPN and white dwarfs is represented by the central stars of old PNe. This prompted us to start a systematic survey of the nuclei of old PNe. We selected apparently very old, faint and extended nebulae whose central stars could be identified. Important sources were the article of Kwitter et al. (1988) and the compilation of nearby PNe by Ishida & Weinberger (1987). The central stars should be far evolved, just entering the white dwarf cooling sequence. First results on interesting stars were reported in Schönberner & Napiwotzki (1990; Paper I) and Napiwotzki & Schönberner (1991a; Paper II). A spectral classification of the complete sample of 38 CSPN is provided in Napiwotzki & Schönberner (1995; Paper III). It

turned out that 28 central stars have a hydrogen-rich surface composition and that only seven were hydrogen-poor. The ratio of hydrogen-rich and -poor objects in our sample of central stars just entering the white dwarf sequence amounts to 4:1, in good agreement with the previous investigations of Liebert (1986) and Méndez (1991) mentioned above. Our result indicates that the ratio of H-rich and H-poor objects remains approximately constant during the evolution from the central star phase to the white dwarf cooling sequence, contrary to what is expected from the Fontaine & Wesemael (1987) scenario. Since this finding is of fundamental meaning for our understanding of many aspects of white dwarf evolution, we will present here the results of a model atmosphere analysis of our central stars. This will allow us to determine their precise evolutionary status. We will in this paper concentrate on the hydrogen-rich central stars, which are the key for our understanding of the pre-white dwarf evolution. Analyses of hydrogen-poor Wolf-Rayet CSPN were recently carried out by Leuenhagen et al. (1996) and Koesterke & Hamann (1997). A review on the properties of PG 1159 stars is given by Dreizler et al. (1995a). Prior to our survey only three analyses of high gravity CSPN were published: A 7 (Méndez et al. 1981), NGC 7293 (Méndez et al. 1988a), EGB 6 (Liebert et al. 1989). Our much enlarged sample now allows a more meaningful investigation of the stellar evolution in this region of the HR diagram.

This paper is organized as follows. We start with a description of the observations and their analysis in Sect. 2 and 3, respectively. The results of the model atmosphere analysis are presented and the evolutionary status of the CSPN is discussed in Sect. 4. The evolution of the helium abundance of hydrogen-rich central stars and white dwarfs is described and compared to theoretical expectations in Sect. 5. The article finishes with conclusions in Sect. 6. We will use the results presented in this article to discuss the question of the PNe distance scale in Paper V of this series.

2. Observations and data reduction

A description of the sample selection and observational details was already given in Paper III. Therefore we will provide here only a cursory overview and details on additional observations.

Spectroscopic observations were performed with the 3.5 m telescope of the Calar Alto Observatory/Spain and the Cassegrain TWIN spectrograph. We performed three runs with low resolution set-ups (October 1989, September 1990, and July 1991). Medium resolution follow-up observations were performed in July 1992, July 1995, and October 1995. The resolution of the low resolution spectra ranges from 5 to 8 Å. Details on the first four runs are provided in Paper III.

The July 1995 and the October 1995 runs used identical set-ups. Grating T 05 in the blue and T 09 in the

red yielded a dispersion of 36 Å/mm. Tek CCDs #11 and #12 with 1024×1024 pixels of size $22\text{ }\mu\text{m}$ were used. The resulting spectral resolution, as measured from the He and Ar lines of the comparison spectra, amounts to $1.5 \dots 1.8\text{ }\text{\AA}$ (FWHM). While we always exposed the region from $5600\text{ }\text{\AA}$ to $6800\text{ }\text{\AA}$ in the red, we needed two grating angle settings to cover the spectral range from $3700\text{ }\text{\AA}$ to $5400\text{ }\text{\AA}$ in the blue channel. However, we did not always get spectra for both ranges. The data reduction follows standard procedures and is identical to that described in Paper III. Let us only remark that we tried to correct for the nebula (and night sky) emission lines. For PNe with moderate line strengths and smooth density distributions this worked well. In cases of PNe with high surface brightness and/or strong spatial inhomogeneities contamination by nebular emission lines remained (either insufficient subtraction or overcorrection). Examples are NGC 6720 and HaWe 5. In these cases the cores of the stellar Balmer lines ($\text{H}\alpha$ and $\text{H}\beta$ most severely) and the $\text{He II } 4686\text{ }\text{\AA}$ line may be corrupted.

We have added the CSPN PHL 932 and the hot DAO white dwarf HZ 34 from Bergeron et al. (1994) to our original sample (Paper III). On the other hand we didn't analyse the spectra of Sh 2-176 and IW 2 from Paper III, because their quality is just good enough for a reliable classification but is too poor for a reasonable analysis. In the case of WeDe 1 (WDHS 1) we based our analysis on the spectrum taken by Liebert et al. (1994), because it's signal-to-noise ratio is higher than that of our spectrum.

3. Model atmosphere calculations and fit procedure

We calculated hydrogen and helium composed model atmospheres with the NLTE code developed by Werner (1986). Basic assumptions are those of static, plane-parallel atmospheres in hydrostatic and radiative equilibrium. In contrast to the atmospheres commonly used to analyze DA white dwarfs, we relax the assumption of local thermal equilibrium (LTE) and solve the detailed statistical equilibrium instead of the Saha-Boltzmann equations. As described in Werner (1986), the accelerated lambda iteration (ALI) method is used to solve the set of non-linear equations.

The analysis of white dwarfs is usually the domain of model atmospheres in LTE. It is assumed that deviations from LTE are kept small by the high densities in white dwarf atmospheres. Model atmospheres which drop the LTE assumption are somewhat loosely called non-LTE (NLTE) atmospheres. A detailed check of the validity of the LTE assumption was presented in Napiwotzki (1997). It could be shown that LTE is a very good approximation for the "classical" DA white dwarfs with temperatures below 40000 K . However, the situation is completely different for typical white dwarf central stars ($T_{\text{eff}} = 100000\text{ K}$, $\log g \approx 7.0$). The higher temperature and lower gravity

causes large deviations between both types of model spectra. Therefore it is necessary to use NLTE model atmospheres for the analysis of these stars.

Levels and lines are included in NLTE up to $n = 16$ for hydrogen, $n = 32$ for He II , and $n = 9$ for He I . He I levels with $n = 5$ to 9 were merged into one singlet and one triplet level for every principal quantum number. The $n = 5$ levels were split with respect to their angular quantum number for the subsequent spectrum synthesis. Line blanketing by the Stark broadened lines is taken into account consistently for hydrogen, He II lines and the resonance series of He I . The synthetic spectra are computed with the extended VCS broadening tables (Vidal et al. 1970) provided by Schöning & Butler (1989; priv. comm.) and Lemke (1997) for hydrogen and He II . We used the He I line broadening tables computed by Barnard et al. (1974), Shamey (1964) and Barnard et al. (1969). Profiles of the isolated He I lines $5016\text{ }\text{\AA}$ and $5876\text{ }\text{\AA}$ were computed according the prescription of Griem (1974).

Pressure dissolution of the higher levels is described by the Hummer & Mihalas (1988) occupation probability formalism following the NLTE implementation by Hubeny et al. (1994). In contrast to our analysis of EUV selected DA white dwarfs (Napiwotzki et al. 1999) we did *not* increase the critical ionizing field β_{crit} adopted to calculate the occupation probability by a factor two as proposed by Bergeron (1993). The motivation of Bergeron was not a flaw in the Hummer & Mihalas (1988) formalism, but a compensation for the inadequacy of the standard Stark broadening theory when line wings overlap. This improved the agreement with experimental measurements and the fits to DA white dwarfs in the Bergeron et al. (1992) sample. Finley et al. (1997) reported also better fit quality for hotter EUV selected white dwarfs. However, the central stars analysed here have even higher temperatures, and their gravities are lower by typical one or two dex in comparison to the stars discussed in Bergeron (1993) and Finley et al. (1997). It is by no means clear if the correction factor is a valid approximation in the case of our CSPN. Thus we preferred to leave the original value of the critical ionizing field β_{crit} unchanged. From our experience with the EUV selected DA white dwarfs analysed by Napiwotzki et al. (1999) we estimate offsets of the order 0.1 dex in gravity and 2% for T_{eff} when compared to an analysis, which applies this correction factor.

Our NLTE model grids have to cover wide ranges in temperature ($30000\text{ K} \leq T_{\text{eff}} \leq 300000\text{ K}$), gravity ($4.75 \leq \log g \leq 8.75$), and helium abundance (from pure hydrogen up to $n_{\text{He}}/n_{\text{H}} = 3$). Thus, to keep computational effort within reasonable limits, we didn't compute every model in this 3D-mesh, but only the needed ones.

Due to the common lack of other temperature indicators both, effective temperature and gravity, must be determined from the Balmer lines. For DA white dwarfs this was successfully done by simultaneous line profile fitting of all available Balmer lines (e.g. Bergeron et al. 1992; Napi-

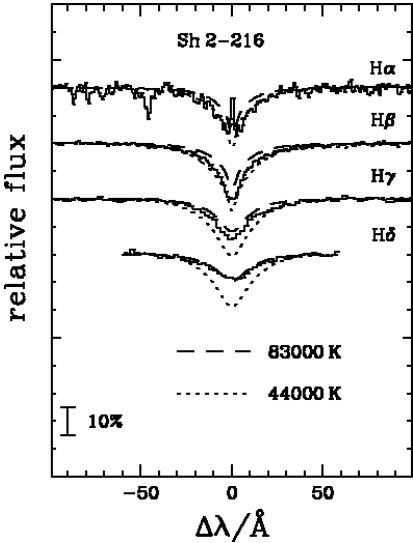


Fig. 1. Model spectra calculated for two different temperatures are compared to the Balmer lines of LS V+46 21, the central star of Sh 2-216

wotzki et al. 1999). Generally the observed line profiles are well reproduced by model spectra with the optimum parameters.

However, this method failed for nearly all hydrogen-rich central stars of old PNe (Napiwotzki 1992; Napiwotzki & Rauch 1994): no consistent fit to the Balmer lines ($H\alpha$ to $H\delta$ were used) was possible. A strong trend is present: fitting of higher Balmer lines yields higher temperatures. This effect is demonstrated for the spectrum of the white dwarf central star Sh 2-216 in Fig. 1. While a high T_{eff} model (83000 K) fits the $H\delta$ line, only 44000 K are needed to fit the $H\alpha$ line. This difference causes serious problems for the interpretation of the evolutionary status of white dwarf central stars. The previous investigation carried out by Méndez et al. (1988a) restricted the analysis to one Balmer ($H\gamma$) line only and thus failed to recognize this discrepancy.

Napiwotzki (1993a) argued that the high temperature derived from the highest Balmer line available ($H\delta$ or $H\epsilon$ respectively) is closest to the real temperature of the white dwarf central stars. Important evidence came from the analysis of the sdO star BD+28°4211. Its spectral appearance is very similar to central stars of old PNe. As can be seen from Fig. 3 in Napiwotzki (1993a) the Balmer line problem is of similar strength as it is in the central star of Sh 2-216 (Fig. 1). Since BD+28°4211 is relatively bright ($V = 10.5$) we were able to obtain a high-resolution spectrum and detected the 5876 Å line of neutral helium (Fig. 4 of Napiwotzki 1993a). HeI lines are very sensitive temperature indicators in this parameter range. We derived a best fit with $T_{\text{eff}} = 82000$ K in excellent agreement with the temperature determination from the HeI line (85000 K).

Napiwotzki & Schönberner (1993) and Napiwotzki & Rauch (1994) discussed possible reasons of the Balmer line problem: wind effects, magnetic fields, pressure ionization and line quenching, deficits in the line broadening theory, and modifications of the atmospheric structure due to line blanketing of heavy elements. The authors concluded that none of these effects is sufficient to explain the Balmer line problem. Kubát (1995) found a moderate sphericity effect on $H\alpha$ and, to a lesser extent, on $H\beta$, too, for pre-white dwarfs with $\log g \approx 6$. These effects are considerably weaker for larger gravity and too small to account for the Balmer line problem.

Finally, Werner (1996) presented the likely solution of this problem. He demonstrated that the inclusion of Stark broadening for C, N, and O lines can have a strong influence on the atmospheric structure of very hot hydrogen-rich stars. It is likely that the effect on the emergent spectrum is pronounced enough to solve the Balmer line problem. An application of his model atmospheres on BD+28°4211 gave good agreement with the observed spectrum, if the parameters of Napiwotzki (1993a) were used. Werner's results confirm Napiwotzki's (1993a) sophisticated guess that the temperatures derived from the highest Balmer lines are the most reliable, close to the "real" temperature of the central stars. The reason for this behavior is evident in Fig. 1 of Werner (1996), which displays the temperature structure of model atmospheres computed with different treatment of line opacity. The inclusion of Stark broadened CNO lines causes a strong modification of the temperature structure in the atmospheric layers, where $H\alpha$ and $H\beta$ are formed, while the change in the deeper layers, where $H\delta$ and $H\epsilon$ are formed is negligible.

However, to apply this procedure the abundances of C, N, and O need to be known which is not the case for our sample. In addition the computation of a NLTE model grid accounting for the influence of C, N, and O in the above described manner requires very large amounts of computer time, hence we analysed the CSPN with our atmospheres containing only H and He. Since the Balmer line fits result in the same gravity for every Balmer line (within the error limits) we used the following recipe: g was computed from the average of all Balmer lines and T_{eff} was derived from the fit of $H\delta$ (and $H\epsilon$ if available) with g fixed at the average value. The temperatures derived in our early analyses (Napiwotzki & Schönberner 1991b and partly in Napiwotzki 1993b) are often too low, because we could not use the $H\delta$ line at that time due to reduction problems. All our new analyses now include this line and the discrepant cases discussed in Pottasch (1996) with Zanstra temperatures much higher than our analysis results are now resolved.

The line fits were performed with the least-square algorithm described in Bergeron et al. (1992). The observed and theoretical Balmer line profiles are normalized to a linear continuum in a consistent manner. Wavelength shifts

are determined with a cross-correlation method and applied consistently to each complete spectrum. The synthetic spectra are convolved to the observational resolution with a Gaussian and interpolated to the actual parameters with bicubic splines, and interpolated to the observed wavelength scale.

The atmospheric parameters are then determined by minimizing the χ^2 value by means of a Levenberg-Marquardt steepest descent algorithm (Press et al. 1992). Finally, an estimate of the internal errors can be derived from the covariance matrix. In contrast to Bergeron et al. (1992), we estimate the noise of the spectra (σ) used for the χ^2 fit from the neighboring continuum of each line. The S/N is adopted to be constant throughout the line. Line cores, which show some remaining contamination from the nebula, were excluded from the fits.

In our investigation of EUV selected DA white dwarfs (Napiwotzki et al. 1999) we showed that the internal errors are usually much smaller than the real observational scatter as inferred from a comparisons of independent analysis. We used the data collection of Napiwotzki et al. (1999) to derive a more realistic estimate of observational errors. For this purpose we binned the data into 5000 K intervals, determined the scatter, and performed a simple linear fit with $\log T_{\text{eff}}$ as independent variable. The results are

$$\frac{\sigma(T_{\text{eff}})}{T_{\text{eff}}} = -0.0995 + 0.0273 \cdot \log T_{\text{eff}} \quad (1)$$

$$\sigma(\log g) = -0.8673 + 0.2130 \cdot \log T_{\text{eff}} \quad (2)$$

A moderate extrapolation is necessary to apply these fits to our CSPN analyses. We took a conservative approach and assumed that these σ values correspond completely to the external errors and added them quadratically to the internal errors derived with the fit procedure.

4. Results and evolutionary status of the central stars

The results of our analysis are summarized in Table 1. The fits to the Balmer lines and helium lines are displayed in Figs. 4 to 7. Due to the Balmer line problem discussed above we derived usually different temperatures from the individual Balmer lines. The individual values are indicated in the plots. The spectra are grouped according to their spectral appearance. Within a plot the spectra are displayed in order of increasing galactic longitude.

A $T_{\text{eff}}-g$ diagram with the results is given in Fig. 2. For comparison evolutionary tracks of post-AGB stars computed by Blöcker (1995), Schönberner (1983), Koester & Schönberner (1986) labeled with the remnant mass are plotted as solid lines. The dashed low mass tracks are taken from the computations of Driebe et al. (1998). They represent the evolution of stars whose hydrogen-rich envelope was stripped away by a companion during the (first) red giant branch phase (Kippenhahn et al. 1967; Iben &

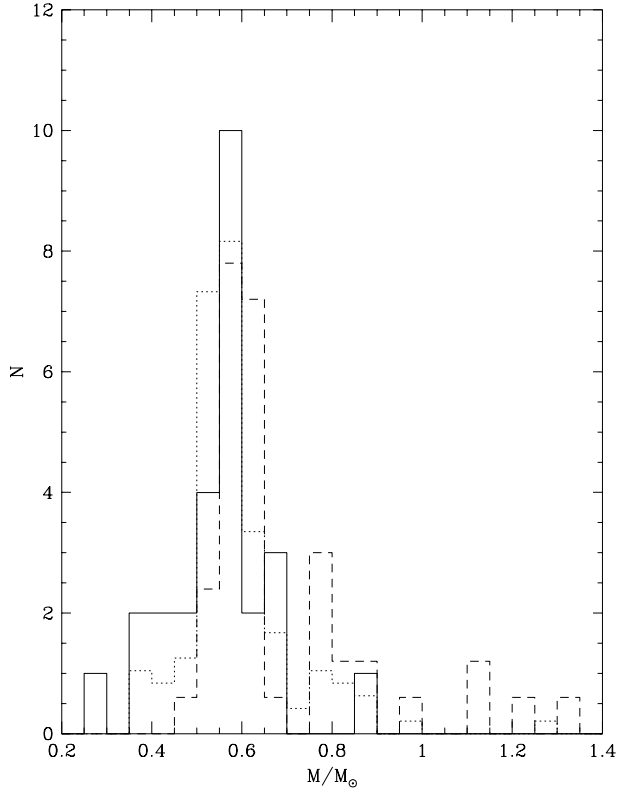


Fig. 3. Mass distribution of the central stars of old PN (solid histogram) compared to two mass distributions obtained from analyses of hot DA white dwarfs (Bergeron et al. 1992, dotted histogram; Napiwotzki et al. 1999, dashed histogram)

Tutukov 1986). The remaining mass is too low for the ignition of helium burning and the star will eventually become a low mass white dwarf with a helium core. In the remainder of this paper we will term this scenario “post-RGB evolution” for the sake of simplicity.

The dotted track describes the evolution of a $0.524M_{\odot}$ post-early AGB (post-EAGB) track from Blöcker (1995). This star suffers from two late helium flashes, which are responsible for the extended loops, and eventually enters the white dwarf domain on a track very similar to that of the $0.546M_{\odot}$ model. Helium burning stars with significantly lower masses will never enter the (early) AGB and thus never produce a PN (AGB manqué evolution; cf. Dorman et al. 1993).

The new analyses are plotted as filled symbols. Our new results are supplemented by data taken from the literature (open symbols) for hydrogen-rich CSPN and DA/DAO white dwarfs. Hydrogen-poor objects are represented by PG 1159 stars, DO white dwarfs, and O(He) post-AGB stars. Stellar parameters and references are provided in Table A.2 and Table A.1 in the Appendix. The symbols of stars with a known PN are encircled. Although analyses of hydrogen-poor Wolf-Rayet CSPN exist (Koesterke & Hamann 1997), which indicate that

Table 1. Parameters of the hydrogen-rich central stars. T_{eff} was derived from the fit of $\text{H}\delta$ (+He) as described in the text. The CSPN are denoted by their PG designation and by their common names. Masses were derived from the comparison with the evolutionary tracks in Fig. 2

PG	Name	T_{eff} (K)	$\log g$ (cm s^{-1})	$\log n_{\text{He}}/n_{\text{H}}$	M (M_{\odot})	d_{NLTE} (pc)	R (pc)	t_{kin} (10^3 yrs)
025.4–04.7	IC 1295	90100 ± 6200	6.66 ± 0.30	-1.31 ± 0.12	0.51 ± 0.04	715	0.16	7.6
027.6+16.9	DeHt 2	117000 ± 6300	5.64 ± 0.22	-0.79 ± 0.12	$0.64^{+0.13}_{-0.06}$	2382	0.54	27
030.6+06.2	Sh 2-68	95800 ± 9300	6.78 ± 0.32	-1.02 ± 0.21	0.55 ± 0.03	1054	1.02	200
034.1–10.5	HDW 11	68100 ± 9400	6.38 ± 0.31	-1.23 ± 0.24	0.39 ± 0.03	1176	0.13	6.6
036.0+17.6	A 43	116900 ± 5500	5.51 ± 0.22	-0.14 ± 0.22	$0.68^{+0.13}_{-0.08}$	2649	0.51	25
036.1–57.1	NGC 7293	103600 ± 5500	7.00 ± 0.22	-1.43 ± 0.15	0.57 ± 0.02	291	0.69	28
047.0+42.4	A 39	117000 ± 11000	6.28 ± 0.22	-0.85 ± 0.10	0.57 ± 0.02	1931	0.81	22
060.8–03.6	NGC 6853	108600 ± 6800	6.72 ± 0.23	-1.12 ± 0.09	0.56 ± 0.01	436	0.42	13.4
063.1+13.9	NGC 6720	101200 ± 4600	6.88 ± 0.26	-1.14 ± 0.09	0.56 ± 0.02	1088	0.20	2.6
066.7–28.2	NGC 7094	125900 ± 7700	5.45 ± 0.23	-0.04 ± 0.14	$0.87^{+0.20}_{-0.23}$	2246	0.51	11.1
072.7–17.1	A 74	108000 ± 15000	6.82 ± 0.27	-1.94 ± 0.25	0.56 ± 0.03	1673	4.52	170
077.6+14.7	A 61	88200 ± 7900	7.10 ± 0.37	-1.58 ± 0.18	0.55 ± 0.05	1380	0.67	22
111.0+11.6	DeHt 5	76500 ± 5800	6.65 ± 0.19	<-2.69	0.44 ± 0.04	512	0.66	129
120.3+18.3	Sh 2-174	69100 ± 3000	6.70 ± 0.18	-2.55 ± 0.13	0.43 ± 0.03	556	0.81	40
124.0+10.7	EGB 1	147000 ± 25000	7.34 ± 0.31	<-1.66	0.65 ± 0.05	653	0.41	20
125.9–47.0	PHL 932	35000 ± 900	5.93 ± 0.12	-1.53 ± 0.05	0.28 ± 0.01	235	0.16	7.7
128.0–04.1	Sh 2-188	102000 ± 32000	6.82 ± 0.60	-1.27 ± 0.64	0.56 ± 0.07	965	0.88	22
148.4+57.0	NGC 3587	93900 ± 5600	6.94 ± 0.31	-1.07 ± 0.13	0.55 ± 0.03	1269	0.52	12.8
149.4–09.2	HDW 3	125000 ± 28000	6.75 ± 0.32	-0.87 ± 0.37	0.58 ± 0.03	1451	1.90	93
156.3+12.5	HDW 4	47300 ± 1700	7.93 ± 0.16	<-3.59	0.64 ± 0.07	246	0.063	3.1
156.9–13.3	HaWe 5	38100 ± 1500	7.58 ± 0.20	<-2.21	0.51 ± 0.04	420	0.035	1.7
158.5+00.7	Sh 2-216	83200 ± 3300	6.74 ± 0.19	-1.95 ± 0.06	0.49 ± 0.03	185	2.69	660
158.9+17.8	PuWe 1	93900 ± 6200	7.09 ± 0.24	-1.70 ± 0.20	0.56 ± 0.03	695	2.02	73
197.4–06.4	WeDe 1	141000 ± 19000	7.53 ± 0.32	<-1.70	0.68 ± 0.07	968	2.17	133
204.1+04.7	K 2-2	67000 ± 11000	6.09 ± 0.24	-1.55 ± 0.15	0.38 ± 0.04	628	0.66	65
215.5–30.8	A 7	99000 ± 18000	7.03 ± 0.43	-1.49 ± 0.37	0.57 ± 0.05	705	1.30	63
219.1+31.2	A 31	84700 ± 4700	6.63 ± 0.30	-1.53 ± 0.13	0.48 ± 0.04	988	2.32	65
	HZ 34	90800 ± 3900	6.60 ± 0.20	-1.59 ± 0.09	0.51 ± 0.03			

these stars are counterparts of the luminous hydrogen-rich CSPN analyzed by Méndez et al. (1988a) there is no simple way to place them into our $T_{\text{eff}}-g$ diagram, because a g determination is not possible without further assumptions.

The central stars of old PNe fill nicely the reported “gap” of the hydrogen-rich sequence. A continuous hydrogen-rich sequence from the central star to the white dwarf region is revealed, and therefore evolutionary scenarios claiming a hydrogen-poor stage of all (or most) pre-white dwarfs (Fontaine & Wesemael 1987) can be ruled out. The gap in the hydrogen-rich sequence can be traced back to selection effects. Some of the hottest hydrogen-rich white dwarfs in the Palomar-Green survey (Green et al. 1986), the most important source of faint blue stars until recently, were originally misclassified as sdO or sdB stars (cf. Jordan et al. 1991, Liebert & Bergeron 1995). It is much easier to pick out the peculiar hydrogen-poor PG 1159 stars and DO white dwarfs. In addition, previous analysis of very hot DA or DAO white dwarfs tended to produce too low temperatures. This is probably caused by the neglect of NLTE effects and the Balmer line problem

in these stars (cf. the discussion in Liebert & Bergeron 1995).

We determined masses of the central stars by interpolating in the evolutionary tracks in Fig. 2. The values are provided in the sixth column of Table 1. Error limits were estimated by propagating the errors of temperature and gravity. Additional errors may result from the adopted tracks. This is not a major problem for stars lying on the post-AGB tracks. However, the mass determination of stars, which cannot be explained by standard post-AGB evolution, might be wrong, if the star didn’t evolve according to the adopted scenario but has a completely different history. The individual cases are discussed below.

The resulting mass distribution (binned over $0.05 M_{\odot}$) is shown in Fig. 3. For comparison we show mass distributions derived for hot DA white dwarfs (Bergeron et al. 1992; Napiwotzki et al. 1999) scaled down to the number of analyzed CSPN. The Bergeron et al. mass distribution was redetermined with the Blöcker (1995) and Driebe et al. (1998) evolutionary tracks. The Napiwotzki et al. (1999) analysis already applied these tracks. The Bergeron et al. sample contains mainly relatively cool DA white dwarfs in

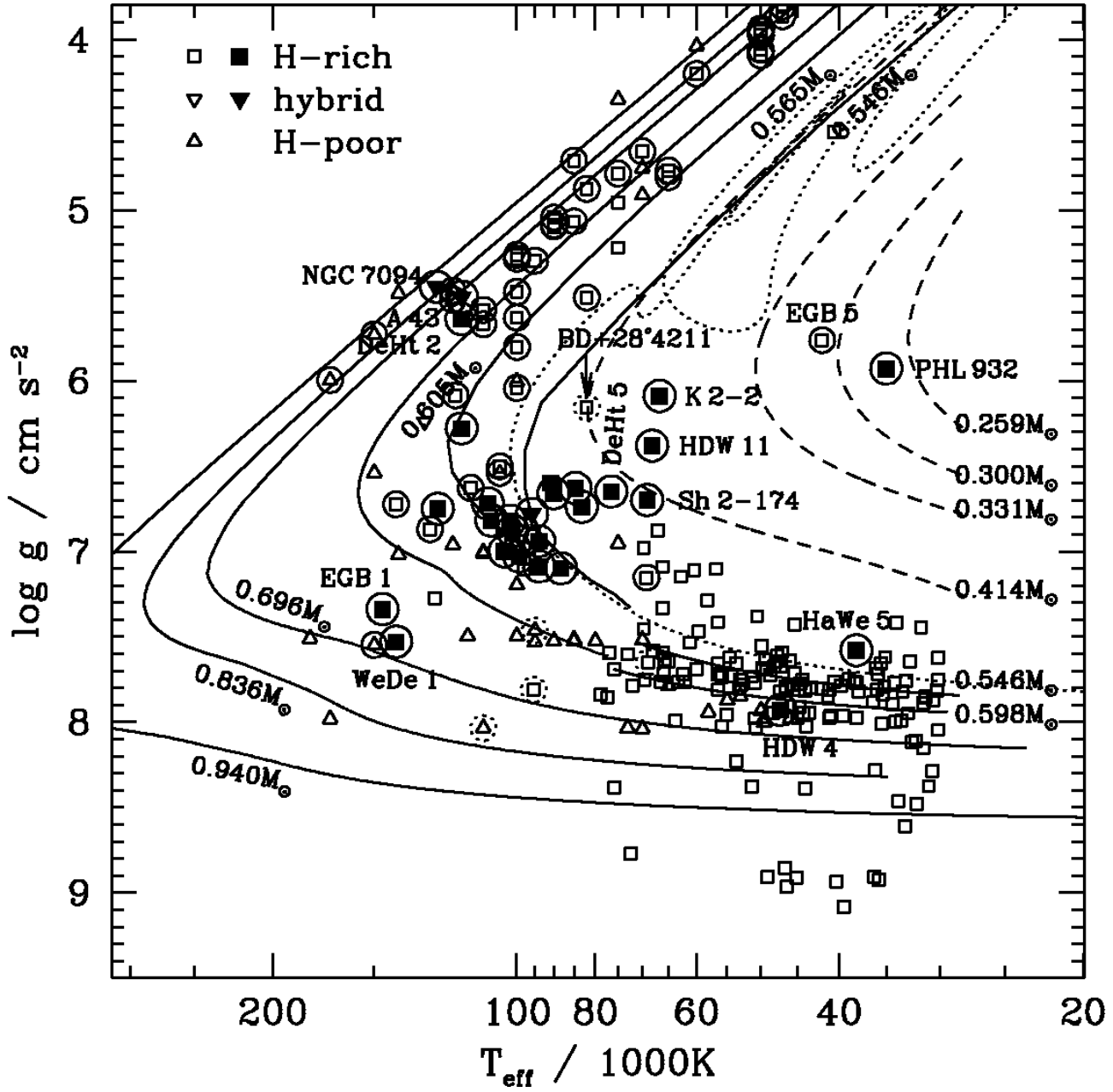


Fig. 2. $T_{\text{eff}}-g$ diagram with the results of the new analyses plotted as filled symbols. These data are supplemented by results taken from literature (open symbols). Hydrogen-rich objects are marked by squares, hydrogen-poor by triangles. Central stars are encircled, a dashed circle is used for suspected PNe. Since the parameters from literature are sometimes rounded to identical values the positions of these stars are shifted by small random values. Post-AGB evolutionary tracks are drawn as solid lines, labeled with the mass of the remnant. Dashed lines indicate the post-RGB tracks discussed in the text. The $0.524M_{\odot}$ post-EAGB track is drawn as dotted line

the temperature interval $15000 \text{ K} \leq T_{\text{eff}} \leq 30000 \text{ K}$, while the Napiwotzki et al. sample is EUV selected and covers $25000 \text{ K} \leq T_{\text{eff}} \leq 55000 \text{ K}$. The CSPN mass distribution peaks in the $0.55 \dots 0.60$ interval, similar to the white dwarf distributions. Note, however, that the low mass tail is more pronounced than in the DA studies. Napiwotzki et al. described that EUV selected samples do select *against* low mass white dwarfs, which explain the deficiency in

their study. It is likely that slowly evolving low mass stars are *preferentially* detected in extended, low density nebulae. However, we don't expect a strong selection against high mass CSPN in our sample, because the evolution of massive central stars slows down and becomes comparable to that of low mass stars, when low luminosities are reached. Blöcker (1995) claims that high mass CSPN evolve even slower than $0.6M_{\odot}$ remnants in this phase.

However, this depends on the treatment of AGB mass loss (cf. discussions in Blöcker 1995 and Vassiliadis & Wood 1994).

Since the mean might be heavily biased by few objects with extreme masses, it is not very useful for the comparison of white dwarf mass distributions. Finley et al. (1997) proposed a Gaussian fit of the mass peak as a robust estimate of the distribution peak. Due to small number statistics and/or the high fraction of low mass stars the width of the best fitting Gauss curve is relatively high: $0.14M_{\odot}$. This is twice the value typically found in the DA investigations and casts some doubt on the fit quality. However, we redid the fit with the width held fixed at $0.07M_{\odot}$ and computed a peak mass only $0.001M_{\odot}$ higher. This convinced us that the derived peak mass of $0.55M_{\odot}$ is reliable. The corresponding value for the Bergeron et al. (1992) sample ($0.56M_{\odot}$) and for the Napiwotzki et al. (1999) sample ($0.59M_{\odot}$) are in agreement. Stasińska et al. (1997) determined the mass distribution of CSPN from a distant independent approach using the nebular $H\beta$ flux, the angular radius, the expansion velocity, and the stellar V magnitude. This method is based on a simple model of the PN evolution (Górny et al. 1997). Stasińska et al. find a narrow mass distribution with $\approx 80\%$ of all objects in the range $0.55 \dots 0.65M_{\odot}$. The median of the sample amounts to $0.60M_{\odot}$. However, this value is slightly dependent of the adopted nebula mass in their PN model. Although this is a completely different approach it is in good agreement with our results for the central stars of old PNe. However, Stasińska et al. find no central stars with masses below $0.55M_{\odot}$. This might partly be explained by their selection criteria, which prefer brighter, younger PNe.

We have used the values of effective temperature, gravity, and mass given in Table 1 and the apparent magnitudes given in Paper III to calculate the distances d_{NLTE} of the CSPN. The results are provided in Table 1 together with the radius R and the kinematical age t_{kin} of the PNe computed from the nebular data compiled in Paper III. See Paper V for more details.

4.1. The DAO stars

Most central stars of old PNe cluster around $T_{\text{eff}} \approx 100000\text{ K}$ and $\log g \approx 7.0$. These are the DAO central stars displayed in Figs. 4 and 5. Among this group the central stars of well known PNe like NGC 6720 (the Ring nebula), NGC 7293 (the Helix nebula), and NGC 6853 (the Dumbbell nebula) are found. Another member is the central star of Sh 2-216, the closest known PN. According to the definition of the spectral type DAO the spectra are dominated by the hydrogen Balmer lines, but the $\text{He II } 4686\text{ \AA}$ line and sometimes $\text{He II } 4542\text{ \AA}$ and 5412 \AA are present. Generally these DAO central stars compare well with low mass post-AGB tracks. That's in contrast with the results Bergeron et al. (1994) for field DAO white dwarfs. These stars are cooler and are probably descendants of the extreme hor-

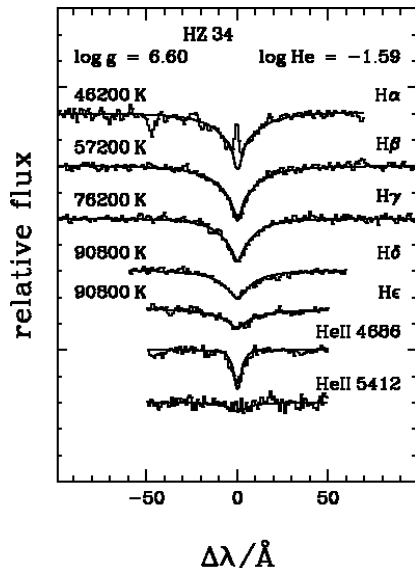


Fig. 6. Our reanalysis of the field DAO white dwarf HZ 34 from the Bergeron et al. (1994) sample

izontal branch (EHB), the so-called AGB-manqué stars, which stay hot during their post-HB evolution and never enter the AGB. Thus we conclude that DAO stars can result from both evolutionary paths. In Sect. 5 we will show that, according to the observational evidence, the DAO phase is simply a transition stage passed by stars entering the DA sequence.

Note that our re-analysis of HZ 34 yields a temperature 10000 K higher than the value given by Bergeron et al. (1994). The new parameters are consistent with a post-AGB nature. Actually this star has parameters very similar to other DAO central stars with a nebula. Therefore it is tempting to speculate about an as yet undetected PN around this star. However, a deep survey for nebula emission performed by Tweedy & Kwitter (1994) ended up with a negative result for HZ 34. Another star with parameters similar to the DAO central stars is the well-known sdO star BD+28°4211. The analysis presented in Napiwotzki (1993a) yielded $T_{\text{eff}} = 82000\text{ K}$, $\log g = 6.2$, and $n_{\text{He}}/n_{\text{H}} = 0.1$. These parameters place BD+28°4211 in a region of the HR diagram, which is consistent with a star either close to the lower mass limit of post-AGB evolution or with post-RGB evolution. Interestingly, Zanin & Weinberger (1997) detected recently a very large, faint emission region with an angular diameter of 5° centered on BD+28°4211, which may possibly be the PN of this star. However, more observational data is needed before one can decide whether this is a chance alignment or really the PN of BD+28°4211.

The coolest DAO white dwarf found in our sample is GD 561, the central star of Sh 2-174. It has an effective temperature of only 69000 K and cannot be explained by standard post-AGB evolution (cf. Fig. 2). The status of GD 561 was already discussed in Tweedy & Napiwotzki

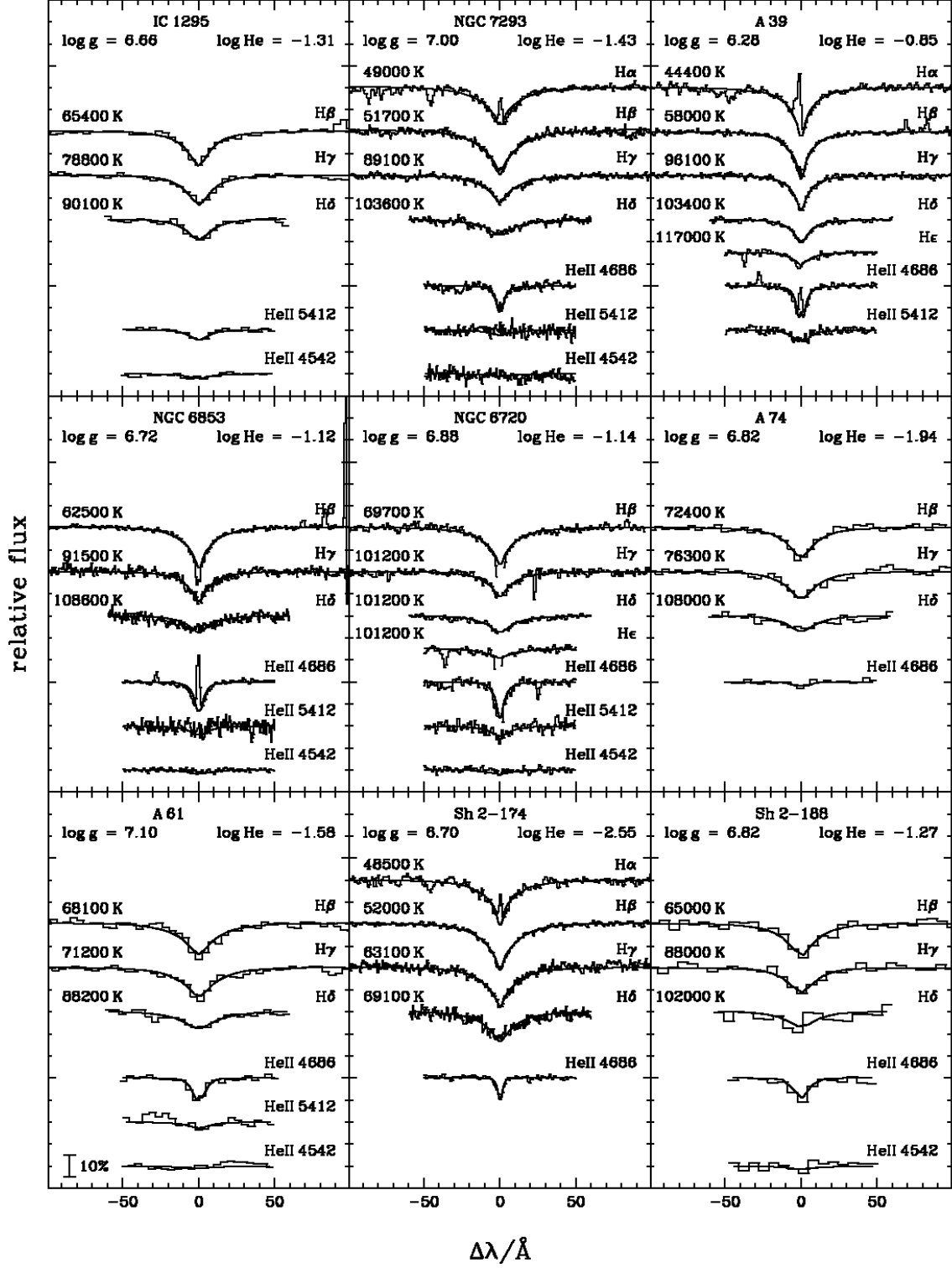


Fig. 4. Spectral fits of DAO central stars. The stars are ordered by increasing galactic longitude

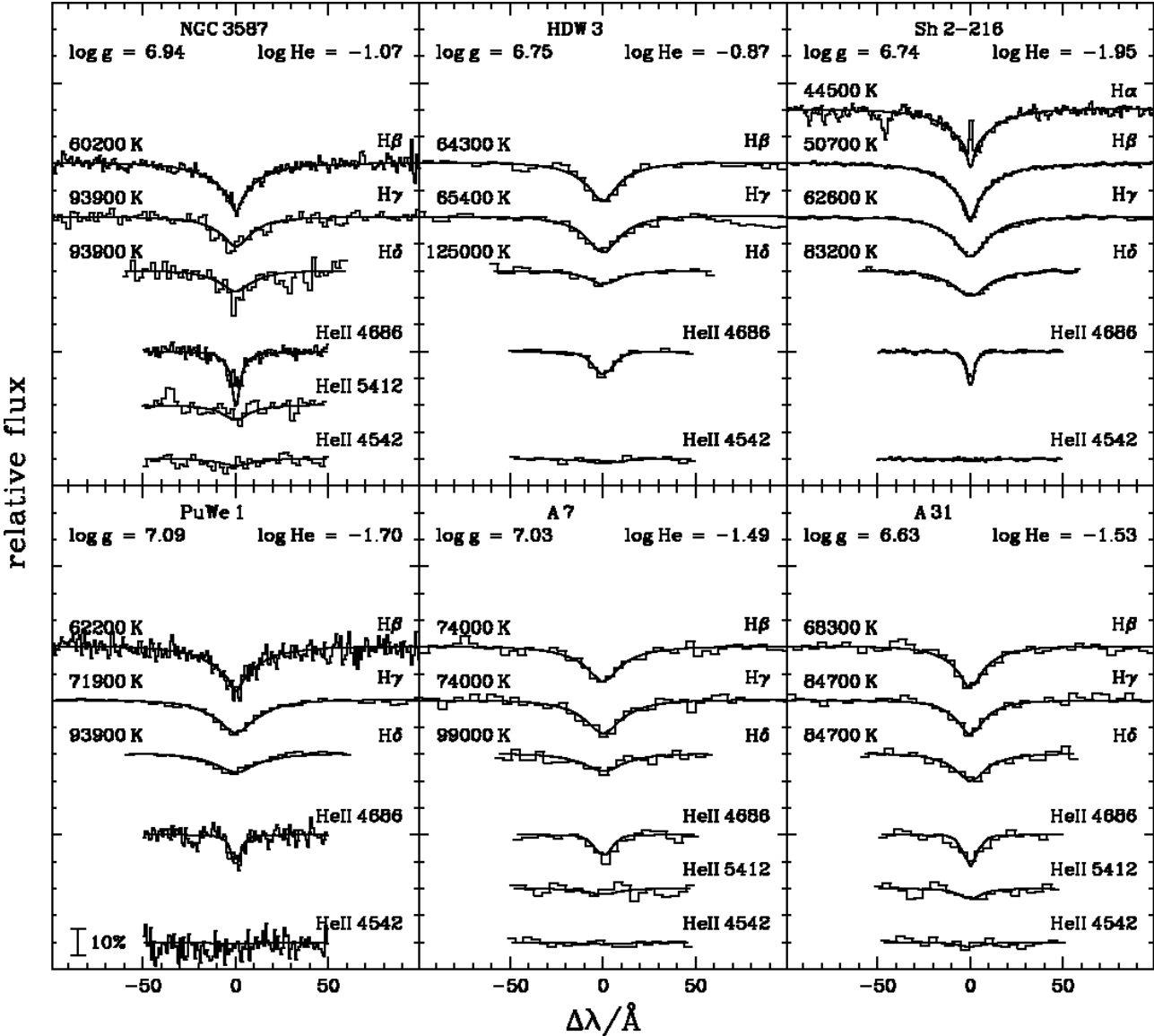


Fig. 5. Spectral fits of DAO central stars (cont.)

(1994). The existence of a PN provides us with constraints on possible evolutionary scenarios. Bergeron et al. (1994) proposed an origin from the extreme horizontal branch (EHB). The parameters of GD 561 can be reproduced by post-EHB evolution (e.g. Dorman et al. 1993). However the PN remains unexplained. Since the horizontal branch evolution lasts $\approx 10^8$ years, any nebula produced on the RGB would be dispersed in the meantime. The mass of the remaining hydrogen-layer ($< 0.01M_\odot$) of EHB stars is much too low to produce a relevant nebula at the end of the horizontal branch stage. Obviously this region of the HR diagram is populated by stars which are not of a post-EHB origin as well.

GD 561 is most likely the outcome of close binary evolution. During the giant stage (on the AGB or RGB) of the central star precursor, it can fill its Roche lobe or

even enclose the companion in its envelope (common envelope evolution). Especially the latter causes heavy mass loss and a modification of the stellar evolution. The result is a hot star inside an expanding shell, which can mimic a normal PN (see e.g. the review of Livio 1993). Tweedy & Napiwotzki (1994) showed that the parameters of GD 561 can be explained by the track of a $0.296M_\odot$ star, which lost its envelope during a common envelope event on the RGB (Iben & Tutukov 1986). However, the evolutionary age ($4 \cdot 10^6$ yrs) predicted by these calculations is uncomfortably large compared with the kinematical age of Sh 2-174 (40000 yrs; Table 1). The new post-RGB tracks of Driebe et al. (1998) provide a much better agreement: the $0.414M_\odot$ track reaches the position of GD 561 within 100000 years after the RGB is left. Note that the PN age estimate is rather uncertain because the expansion veloc-

ity has not been measured. A photometric search for cool companions in the infrared J, H, K bands (Napiwotzki 1995) found a cool companion of GD 561 separated by $\approx 4''$. Furthermore, the preliminary analysis revealed that the central star itself has an infrared excess of $0.^m5$ in K indicating binarity. The system might in fact be a triple one.

4.2. The peculiar central stars K 2-2, HDW 11, and PHL 932

It appears that the CSPN K 2-2 and HDW 11 (Fig. 7) are lower gravity counterparts of GD 561/Sh 2-174. Their positions in the HR diagram (Fig. 2) fit into the post-RGB scenario. Judged from the comparison with the Driebe et al. (1998) tracks their masses are slightly lower ($0.39M_{\odot}$ and $0.38M_{\odot}$ for HDW 11 and K 2-2, respectively) and their theoretical post-RGB ages lie in the range $100000 \dots 200000$ yrs. While the kinematical age of K 2-2 (65000 yrs) is consistent with that prediction, the age of HDW 11 appears to be too low (6600 years). Note that, again, no expansion velocity has been measured for HDW 11 and thus the age was calculated by using the canonical value of 20 km/s. If the expansion is slower the age of HDW 11 might be higher.

While the age determination of HDW 11 might be in marginal agreement with the post-RGB scenario, this is certainly not true for PHL 932. From Fig. 2 we read of a mass of $0.28M_{\odot}$. The age corresponding to the position of PHL 932 is $3 \cdot 10^6$ yrs, the PN age amounts to 7700 yrs only. Although both age determinations are subject to severe uncertainties the discrepancy is so large that this scenario can be ruled out. PHL 932 might be the result of a common envelope event of a star with a degenerate CO core as calculated by Iben & Tutukov (1985; see Iben & Livio 1983 for a review on common envelope evolution). Méndez et al. (1988b) speculated that both stars of the binary might have merged during the common envelope stage. Note that our mass estimate is only valid if PHL 932 is a post-RGB star.

4.3. The hot, high gravity central stars of EGB 1 and WeDe 1

Two high gravity CSPN are distinctly hotter and more massive than typical DAO central stars: EGB 1 ($0.65M_{\odot}$) and WeDe 1 ($0.68M_{\odot}$). Their spectra don't show the He II 4686 Å line indicating that their spectral type is DA. However, due to the high temperature and gravity of these objects the upper limits, which can be derived from our optical spectra are not very stringent: $n_{\text{He}}/n_{\text{H}} < 0.02$ for both stars. Thus the absence of helium lines can already be explained by a modest depletion.

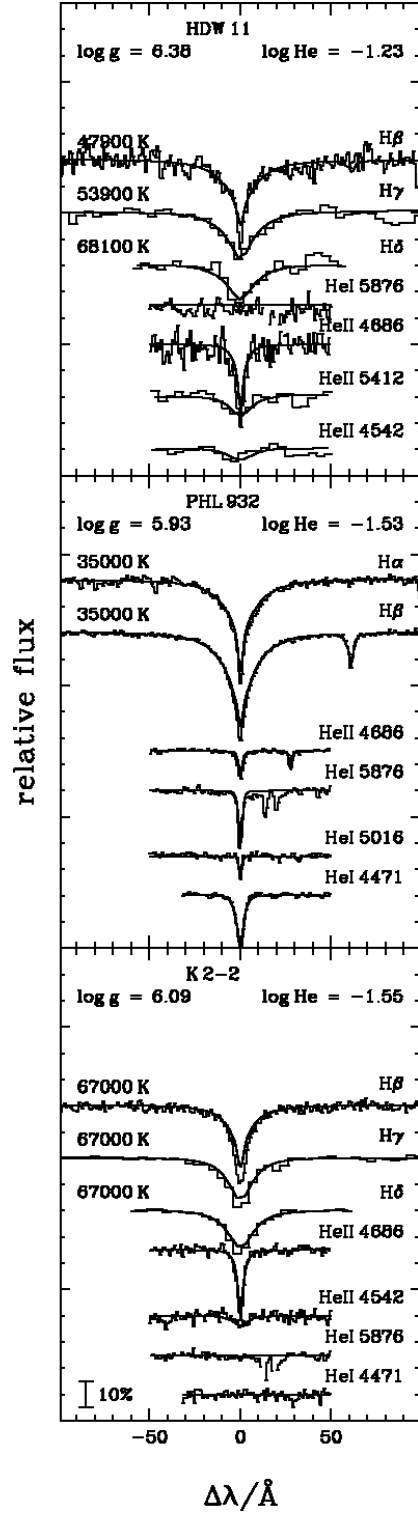


Fig. 7. Spectral fits of the peculiar central stars HDW 11, PHL 932, and K 2-2

4.4. DA central stars

Three cooler DA white dwarfs are present in our sample, too (Fig. 9). DeHt 5 has similar parameters as the DAO white dwarf GD 561/Sh 2-174 although it is slightly hotter

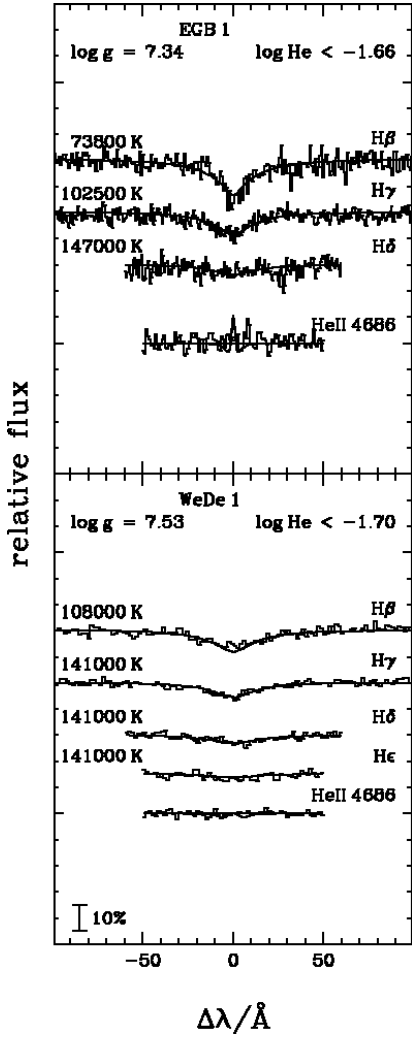


Fig. 8. The hot, high gravity central stars EGB 1 and WeDe 1. The synthetic spectra of the HeII 4686 Å line are computed for the 3σ limit of the helium abundance

($T_{\text{eff}} = 76500$ K vs. 69100 K). This places DeHt 5 closer to the post-AGB tracks (Fig. 2), but a non post-AGB nature of DeHt 5 is more likely. Several scenarios are possible (see discussion of GD 561 above), but DeHt 5 compares well with the post-RGB evolutionary tracks of Driebe et al. (1998). The kinematical age of the PN (129000 years; Table 1) is in good agreement with the post-RGB age (≈ 100000 years) estimated from the $0.414 M_{\odot}$ track.

The DA white dwarfs HDW 4 and HaWe 5 are more mysterious. Their spectral appearance (Fig. 9) and stellar parameters ($T_{\text{eff}} = 47300$ K, $\log g = 7.93$ and $T_{\text{eff}} = 38100$ K, $\log g = 7.58$) resemble ordinary hot DA white dwarfs (cf. Fig. 2). However, the existence of PNe around these stars is very difficult to understand. The theoretical post-AGB ages of 47000 K and 38000 K white dwarfs amount to $\approx 3 \cdot 10^6$ years, and $\approx 6 \cdot 10^6$ years, respectively. That is much older than any PNe found in our sample (cf. Table 1) and one would not expect a PN to survive

that long. Moreover, the nebulae of HDW 4 and HaWe 5 do not appear to be extraordinarily old. Their kinematical ages amount to only 2000 and 3000 years and their surface brightnesses are not atypically low. Actually, the nebula of HaWe 5 is bright enough to contaminate the cores of the H α and H β lines in the central star spectrum (Fig. 9).

We are also not aware of any binary evolution models which can explain the properties of these two central stars and their nebulae, because no scenario is able to produce a remnant which reaches the positions of HDW 4 and HaWe 5 within a reasonable time after departure either from the AGB or RGB (see e.g. Iben & Tutukov 1985; Iben 1986; Iben & Tutukov 1993). The fundamental reason is that the time scales in the white dwarf domain are determined by the gravitational-internal energy of the stellar remnant (Blöcker & Schönberner 1990). If the stellar evolution is abbreviated by a companion stripping off matter from the primary, the structure of the resulting remnant is less compact than that of a normal post-AGB star of the same mass. That means the gravitational-internal energy content is larger and cooling needs even more time.

Since it seems impossible to explain the existence of a PN around these stars, we investigated the hypothesis that the nebula HDW 4 and HaWe 5 only mimic the appearance of a PN. It is well known that white dwarfs in cataclysmic binaries can eject shells during an outburst caused by a thermonuclear runaway after they have accreted a certain amount of hydrogen-rich material from the companion, usually a late type main sequence star. The mass of the ejected material is of the order $10^{-4} M_{\odot}$ (cf. Table 5.7 of Warner 1995), much smaller than the mass of a typical PNe. Sometime after this nova event the expanding shell can become visible as spatially resolved object with a morphology not much different from planetary nebulae (see e.g. Slavin et al. 1995; Tweedy 1995). We inverted the Shklovsky formula (see e.g. Eq. 1 in Paper III) and estimated shell masses of HDW 4 and HaWe 5 of $10^{-3} M_{\odot}$ and $2 \cdot 10^{-4} M_{\odot}$, respectively, consistent with a nova interpretation.

However, nova shells usually have expansion velocities of 500 km/s or higher (see Slavin et al. 1995 and references therein). We have obtained a spectrum of the H α region of HDW 4 with a spectral resolution of 1.63 ± 0.02 Å (FWHM; measured from Gaussian fits of comparison lamp lines). We applied the same fit procedure to the nebular H α line and the N II 6548/84 Å lines and got an average width of 1.85 ± 0.06 Å. If we ignore thermal broadening this provides us with an upper limit on the expansion velocity of $2v_{\text{exp}} < 47$ km/s. That corresponds to typical PN expansion velocities, and is much lower than the usual velocities observed in nova shells, even if one considers projection effects.

Until now we did not detect any binary companion. The low resolution spectra of HDW 4 and HaWe 5 end at 6800 Å and don't display any signs of a cool companion. Ongoing mass accretion from a companion must be very

low if any, because otherwise the atmospheres of HDW 4 and HaWe 5 would be contaminated by helium and heavy elements and would not show the pure hydrogen spectrum we observe. A probable counterpart of our mysterious stars might be the very old nova CK Vul which exploded in 1670. Shara et al. (1985) recovered it as a very faint star inside a faint nebulosity on deep CCD images. From the size of the nebulosity Shara et al. estimated an expansion velocity of 59 km/s, lower than for any other known nova shell. However, a direct measurement of line widths is still lacking. Naylor et al. (1992) took the nova nature of CK Vul into question because the proposed central star doesn't show $H\alpha$ in emission as it is usually observed even in old nova systems (Ringwald et al. 1996). Shara et al. (1985) concluded that any mass transfer in the CK Vul system must virtually have stopped. An infrared investigation gave evidence for cool dust in the system (Harrison 1996). Although observational evidence is spurious it may well be that HDW 4, HaWe 5, and CK Vul belong to the same class of objects. Theoretical calculations (Shara et al. 1993; Prialnik & Kovetz 1995) predict that nova outbursts of white dwarfs with "atypical low masses" of 0.60 or $0.65M_\odot$ (roughly the masses of HDW 4 and HaWe 5) should be very slow and eject high shell masses compared to nova with more "typical" white dwarf masses ($0.91M_\odot$; Webbink 1990). This might explain the observational properties of HDW 4 and HaWe 5 discussed above. However, no definite conclusions are possible without further observational data. A deep IR search for companions in both CSPN will be of special importance.

4.5. Central stars of hybrid spectral type

Our sample contains three hydrogen-rich PG 1159 stars or hybrid CSPN (Sh 2-68, A 43, NGC 7094). Their spectra show a C IV absorption trough in the region of the He II 4686 Å line as it is typical for the hydrogen-poor, carbon- and helium-rich PG 1159 stars (see Dreizler et al. 1995a for a review). However, unlike in PG 1159 stars the Balmer lines are visible, too, which indicates a much higher amount of hydrogen in their atmospheres. The first star of this type, Sh 2-68, was found during our survey of central stars of old PNe (Paper II). Dreizler et al. (1995a) analyzed A 43 and NGC 7094 taking also the lines of C, N, and O into account. They derived $T_{\text{eff}} = 110000$ K and $\log g = 5.7$ for both stars. The agreement with our analysis of A 43 is good, while we derive a significantly higher temperature for NGC 7094. The difference of the Balmer lines of both stars (Fig. 10) indicates that the parameters of these stars cannot be equal. NGC 7094 is likely to be hotter and/or of lower gravity than A 43. HS 2324+3944 is the only star of this class without a PN (Dreizler et al. 1996). A search for a nebula around this star was not successful (Werner et al. 1997).

The hybrid CSPN (hydrogen-rich PG 1159 stars) A 43 and NGC 7094 are placed on the horizontal part of the

post-AGB tracks, where only one other CSPN of our sample is found. All other stars are more evolved. The comparison with the evolutionary tracks yields post-AGB ages smaller than 1000 yrs, which is short compared to the kinematical ages of their PNe (25000 yrs and 11000 yrs for A 43 and NGC 7094, respectively). However, if we consider the error bars and uncertainties of age determinations both ages can in principle brought into agreement. On the other hand their position in the HR diagram, distinct from the other central stars of old PNe, argues for the reality of this age discrepancy. The absence of a PN around HS 2324+3944 ($T_{\text{eff}} = 130000$ K; $\log g = 6.2$; Dreizler et al. 1996) is another argument for the reality of the discrepancy. A 43 and NGC 7094 are good candidates for born again central stars (Schönberner 1979, 1983; Iben et al. 1983), which returned to the AGB after a late thermal flash and repeat the post-AGB evolution, now as helium-burning stars. The result is a seemingly young central star in an old PNe. This explains the age discrepancy we found for the three hybrid stars discussed above. Fittingly, this scenario is often invoked to explain the chemical abundances of PG 1159 stars. However, we found another central star (DeHt 2) with very similar temperature and gravity and an old PNe ($t_{\text{kin}} = 27000$ yrs). If the age discrepancy found for the hybrid central stars is explained by the born-again scenario it should apply to DeHt 2 as well, but no sign of a chemical enrichment of the atmosphere is present. This star might indicate that born again evolution is not necessarily linked to strong chemical processing of the photosphere.

4.6. Comments on individual objects

PNG 025.4-04.7 (IC 1295): The PN is relatively bright and produces severe contamination of the core of $H\beta$ and the He II 4686 Å line. Thus we excluded 4686 Å from the fit and estimated the helium abundance from the He II lines at 5412 Å and 4542 Å. Only the wings of the $H\beta$ line were fitted.

PNG 036.0+17.6 (A 43): The He II 4686 Å region is heavily contaminated by C IV lines and was excluded from the fit.

PNG 036.1-57.1 (NGC 7293): The central star was previously analysed by Méndez et al. (1988a). Their result was $T_{\text{eff}} = 89000$ K and $\log g = 6.9$. The gravity is virtually identical with our value $\log g = 7.00 \pm 0.22$, but their temperature is somewhat lower ($T_{\text{eff}} = 103600 \pm 5500$ K). This is easily explained when one takes into account that $H\gamma$ was the only analysed hydrogen line. Our fit of $H\gamma$ results in $T_{\text{eff}} = 89000$ K, in perfect agreement with the Méndez et al. result.

PNG 047.0+42.4 (A 39): The McCarthy et al. (1997) result $T_{\text{eff}} = 110000 \text{ K}$, $\log g = 6.3$, and $n_{\text{He}}/n_{\text{H}} = 0.11$ agrees with our parameters.

PNG 60.8–03.6 (NGC 6720): The cores of $\text{H}\beta$, $\text{H}\gamma$, and $\text{He II } 4686 \text{ \AA}$ are contaminated by the nebula lines and were excluded from the fit as well as the interstellar Ca II H and K absorption in He. McCarthy et al. (1997) fitted a high resolution spectrum obtained with the HIRES echelle spectrograph of the Keck I telescope and derived a somewhat low temperature of the central star (80000 K). High resolution spectra are certainly useful if one has to deal with bright nebulae. On the other hand it is difficult to reduce the very broad Balmer lines of a $\log g = 7.0$ star, which are distributed over several orders of the HIRES echelle spectrum, without deformation of the line profiles.

PNG 066.7–28.2 (NGC 7094): The $\text{He II } 4686 \text{ \AA}$ region is heavily contaminated by C IV lines and was excluded from the fit.

PNG 125.9–47.0 (PHL 932): The temperatures derived from the Balmer lines and the ionization equilibrium of helium differ by 3000 K . This is certainly caused by our neglect of metal line blanketing. The Balmer line profile differences of the model spectra and the observed spectra are in close agreement to the expectation from the theoretical comparison in Fig. 10 of Napiwotzki (1997). Méndez et al. (1988b) derived $T_{\text{eff}} = 37000 \pm 2000 \text{ K}$, $\log g = 5.5 \pm 0.2$ which is in marginal agreement with our results. Part of the difference might be explained by the use of different model atmospheres and fitting procedures.

PNG 158.9+17.8 (PuWe 1): The McCarthy et al. (1997) derive $T_{\text{eff}} = 110000 \text{ K}$, $\log g = 7.0$, and $n_{\text{He}}/n_{\text{H}} = 0.02$. The temperature is slightly higher than our result (94000 K). See discussion of NGC 6720.

PNG 197.4–06.4 (WeDe 1): WeDe 1 was first announced as a very hot, high-gravity star by Napiwotzki & Schönberner (1991b). A LTE analysis of the moderate quality spectrum available at that time resulted in lower limits on T_{eff} ranging from 100000 K to 200000 K (depending on the adopted helium abundance) and a lower gravity limit of $\log g = 8.5$. A NLTE analysis using a better spectrum and model atmospheres similar to that described in the present paper yielded in $T_{\text{eff}} = 217000 \text{ K}$ and $\log g = 7.35$ (Napiwotzki 1995). Independently, Liebert et al. (1994) performed a LTE analysis and derived $T_{\text{eff}} = 99000 \text{ K} \dots 165000 \text{ K}$, again depending on the adopted helium abundance. Since the quality of the Liebert et al. spectrum is superior to that of our Calar Alto spectrum, we used their spectrum for our analysis. The result is $T_{\text{eff}} = 141000 \pm 32000 \text{ K}$ and $\log g = 7.53 \pm 0.32$. The

dependence of the fit result on the adopted helium abundance is much lower for our NLTE analysis than it is for LTE analyses (cf. Napiwotzki 1997).

PNG 215.5–30.8 (A 7): The McCarthy et al. (1997) result $T_{\text{eff}} = 100000 \text{ K}$, $\log g = 6.6$, and $n_{\text{He}}/n_{\text{H}} = 0.05$ agrees with our parameters.

5. Helium abundances and the onset of diffusion

A wide spread of helium abundances is observed in the atmospheres of hydrogen-rich central stars. Vennes et al. (1988) have shown that helium sinks down due to gravitational settling in the atmospheres of hydrogen-rich white dwarfs. Diffusive equilibrium is reached fast and no visible traces of helium should be present in these atmospheres. Therefore it was considered the most consistent physical picture of DAO white dwarfs that their atmospheres should consist of an extremely thin hydrogen layer on top of the helium envelope. The helium lines should form in the deeper, helium-rich regions. In the context of the Fontaine & Wesemael (1987) scenario of the spectral evolution of white dwarfs DAO stars are transition objects from the helium-rich DO to the hydrogen-rich DA sequence, which have just built up an extremely thin hydrogen-layer. The very thin layer hypothesis can be tested by detailed fits of the $\text{He II } 4686 \text{ \AA}$ profiles. The formation depth of this line is quite different for stratified and homogeneous atmospheres: the line is much broader and shallower in the stratified case. Napiwotzki & Schönberner (1993) demonstrated that the $\text{He II } 4686 \text{ \AA}$ line of Sh 2-216 is well fitted by a homogeneous model atmosphere while a stratified atmosphere could be excluded. Figs. 4 and 5 show also good agreement between the profiles computed from our homogeneous models and those observed for $\text{He II } 4686 \text{ \AA}$. Bergeron et al. (1994) extended this investigation to their DAO sample and found also that the atmospheres of most stars are not stratified. However, they presented one example, PG 1305–017, with a probably stratified atmosphere, which might, indeed, be an object caught during the transition from DO to DA spectral type.

Napiwotzki (1993b, 1995) and Bergeron et al. (1994) noted a correlation between helium abundance and gravity. However, Bergeron et al. (1994) did not consider it to be significant and stressed a stronger correlation with T_{eff} . We search for correlations between the helium abundance and temperature, surface gravity and luminosity in Fig. 12. We combine our results with the DAO analyses of Bergeron et al. (1994) and the CSPN analysis of Méndez et al. (1988a; 1992). All stars of the Méndez et al. sample (with the exception of the peculiar objects EGB 5 and PHL 932) are on the constant luminosity part of the central star tracks. Some stars exhibit helium enrichment by dredge up of nuclear processed material, but none shows a significant depletion below the solar value. If we ignore these luminous Méndez et al. stars, indeed a correlation of

helium abundance with temperature becomes visible (upper panel of Fig. 12), however, not a very good one. On the one hand the hottest stars WeDe 1 and EGB 1 have upper limits below the solar value and on the other hand several of the cooler stars are only mildly depleted. A better correlations is found between $n_{\text{He}}/n_{\text{H}}$ and the surface gravity (middle panel). However, in this case there are exceptions from the general trend present, too. A far better correlation is found between helium abundance and luminosity (lower panel). All stars, whether of post-AGB nature or not, can be explained by one trend line, although the scatter seems to be larger than expected from the observational errors alone. For all stars with a luminosity higher than $\approx 300L_{\odot}$ the helium abundance is close to the “solar” value $n_{\text{He}}/n_{\text{H}} = 0.1$ or above. For stars with lower luminosity the helium abundance steadily decreases with decreasing luminosity. Since effective temperature and surface gravity are related to luminosity it is not surprising that a correlation with temperature is found in a sample with roughly equal gravity (Bergeron et al. 1994), or a correlation with gravity in a sample with roughly equal temperature (Napiwotzki 1993b; 1995). Although intrinsic scatter seems to be present in the correlation of helium abundance with luminosity its existence is remarkable. The observed abundances of heavy elements in hot white dwarfs usually display a more or less stochastical dependence on stellar parameters without any clear trend (cf. Chayer et al. 1995).

Recent theoretical calculations performed by Unglaub & Bues (1998) show that the helium abundances observed in DAO stars can be explained if a reasonable mass loss rate is adopted. Mass loss counteracts the gravitational settling of helium and slows it down, if the strength of the stellar wind is high enough. The mass loss of hot stars is radiatively driven and a strong function of luminosity (e.g. Abbott 1982). Thus a correlation between luminosity and helium abundance is also expected on theoretical grounds. The calculations of Unglaub & Bues (1998) show that the static equilibrium abundances are not reached within typical evolutionary time scales of hot white dwarfs. Therefore the stellar abundances are the result of a dynamical equilibrium between diffusion time scales and the evolution of the star. This might explain why sometimes stars with similar parameters show different photospheric abundances. An example is given by the DA DeHt 5 and the DAO Sh 2-174. DeHt 5 has a slightly higher temperature and slightly lower gravity than Sh 2-174. Thus we would expect the helium abundance of DeHt 5 to be higher than in Sh 2-174, but the spectrum Sh 2-174 shows an easily detectable He II 4686 Å line (Fig. 4) while the line is below the detection limit in the spectrum of DeHt 5 (Fig. 9). However, if the helium abundance is the result of time dependent diffusion it should depend on the previous evolution of the stars. Thus stars with similar parameters but different evolutionary histories can show different abundance patterns. We conclude that today observational ev-

idence and theoretical calculations of the evolution of surface helium abundance show semi-quantitative agreement. What is needed for an improved understanding are self-consistent diffusion calculations taking the stellar evolution into account and an extension of the comparison to as many heavy elements as possible.

6. Conclusions

We presented a NLTE model atmosphere analysis of 27 hydrogen-rich central stars of old PNe. The stars were taken from Paper III in this series, where we provided classifications for a total of 38 CSPN. The analysis of the H-rich CSPN is hampered by the Balmer line problem: for most stars a consistent fit to all Balmer lines was not possible. Generally the highest Balmer line yields the highest temperature. The likely solution of this problem was presented by Werner (1996). He demonstrated that the inclusion of Stark broadening for C, N, and O lines can have a strong influence on the atmospheric structure of very hot hydrogen-rich stars. The lower Balmer lines are most strongly affected and their analysis with standard NLTE model grids yields unreliable temperatures. It is likely that the effect on the emergent spectrum is pronounced enough to solve the Balmer line problem. Since the computation of a NLTE model grid accounting for the influence of C, N, and O in the above described manner requires enormous amounts of computer time, we analyzed the CSPN with our atmospheres containing only H and He and derived T_{eff} from the fit of H δ (or H ϵ if available).

A previously reported gap in the hydrogen-rich evolutionary sequence is filled by our sample and, therefore, shown to result from a selection effect. Taking into account the hot white dwarfs analyzed by Bergeron et al. (1994) we have now a continuous sequence from the CSPN to the white dwarfs. The observational findings are well explained by a two channel scenario with a hydrogen-rich and a hydrogen-poor sequence. It is no longer necessary to invoke an one channel scenario (Fontaine & Wesemael 1987) to explain the spectral evolution of pre-white dwarfs. Note that our findings do not rule out that *some* white dwarfs change their spectral type from DO to DA (see discussions in Fontaine & Wesemael 1997 and Napiwotzki 1998).

Stellar masses were computed from a comparison with evolutionary tracks and a mass distribution for the hydrogen-rich central stars of old PNe was derived. The distribution has a sharp peak centered at $0.55M_{\odot}$. This value and the general shape are similar to the results of previous analysis of hot DA white dwarfs (Bergeron et al. 1992; Finley et al. 1997; Napiwotzki et al. 1999) and of a recent distance independent investigation of PNe (Stasińska et al. 1997). A relatively large fraction of low mass central stars is present in our sample. This might be explained by our selection criteria which tend to prefer

the old and thin nebulae around slowly evolving post-RGB stars.

Although the majority of analyzed stars is well explained by standard post-AGB evolution, there exists a number of stars for which other scenarios have to be invoked. The properties of three stars are probably best explained by born again evolution. Two of these are hybrid CSPN (hydrogen-rich PG 1159 stars), but surprisingly the third star doesn't show any signs of chemical enrichment in its atmosphere. The third hybrid CSPN in our sample (Sh 2-68) has parameters which place it among the group of normal DAO central stars.

The fundamental parameters of five stars are not in accordance with a standard post-AGB evolution. They are likely the outcome of a close binary evolution. Several scenarios are possible. Four stars are reasonably well explained by the evolution of stars whose hydrogen-envelope has been stripped off by a nearby companion during the first red giant branch phase. The remnants will eventually become low mass white dwarfs with a degenerate helium core. Although the post-RGB evolution is considerably slower than post-AGB evolution the existence of low density nebulae around these objects is in accordance with theoretical time scales. The kinematical ages of the observed PNe are consistent with the evolutionary post-RGB age, except for PHL 932, where this scenario is ruled out by a very large discrepancy between predicted post-RGB age and kinematical age of the nebula. Two stars (HDW 4 and HaWe 5) remain mysterious. They resemble ordinary hot DA white dwarfs with evolutionary ages of several million years. However, this large age is in clear contradiction with the presence of a nebula. Close binary evolutionary scenarios do not resolve this discrepancy, because the remnants need several million years after the possible ejection of a nebula to reach the position of HDW 4 and HaWe 5 in the HR-diagram. We speculate that the nebulae of these stars are produced by nova-like events. However, no direct observational evidence can be given in the moment.

Napiwotzki & Schönberner (1993) and Bergeron et al. (1994) have shown that the atmospheres of DAO stars are chemically homogeneous, i.e. not layered. We have shown that a good correlation between helium abundance and luminosity is present. Depletion starts when the stellar luminosity falls below $L \approx 300L_{\odot}$, and the helium abundance steadily decreases with decreasing luminosity. Although the scatter is probably larger than expected from the observational errors alone, the correlation is surprisingly tight considering the more or less stochastic abundance variations usually found in hot white dwarfs (Chayer et al. 1995). The existence of the correlation is in qualitative agreement with recent theoretical calculations of gravitational settling in the presence of a stellar wind (Unglaub & Bues 1998).

Acknowledgements. The author thanks T. Rauch, U. Heber, and S. Moehler who made the medium-resolution observations,

and H. Edelmann, who did the data reduction for one run. I gratefully acknowledge the help of U. Kolb, H. Drechsel, and K. Schenker, who answered many silly questions about cataclysmic binaries. This work was supported by DFG travel grants and by DARA grant 50 OR 96029-ZA.

References

Abbott D.C. 1982, *ApJ* 259, 282
 Barnard A.J., Cooper J., Sheme L.J. 1969, *A&A* 1, 28
 Barnard A.J., Cooper J., Smith E.W. 1974, *JQSRT* 14, 1025
 Barstow M.A., O'Donoghue D., Kilkenny D., Burleigh M.R., Fleming T.A. 1995, *MNRAS* 273, 711
 Bauer F., Husfeld D. 1995, *A&A* 300, 481
 Bergeron P. 1993, in: *White dwarfs: advances in observation and theory*, ed. M.A. Barstow, Kluwer, Dordrecht, p. 267
 Bergeron P., Saffer R.A., Liebert J. 1992, *ApJ* 394, 228
 Bergeron P., Wesemael F., Beauchamp A., et al. 1994, *ApJ* 432, 305
 Blöcker T. 1995, *A&A* 299, 755
 Blöcker T., Schönberner D. 1990, *A&A* 240, L11
 Chayer P., Fontaine G., Wesemael F. 1995, *ApJS* 99, 189
 Dorman B., Rood R.T., O'Connell R.W. 1993, *ApJ* 419, 596
 Dreizler S., Heber U. 1998, *A&A* 334, 618
 Dreizler S., Werner K. 1996, *A&A* 314, 217
 Dreizler S., Werner K., Heber U. 1995a, in: *White dwarfs*, eds. D. Koester & K. Werner, Springer-Verlag, Berlin, Heidelberg, p. 160
 Dreizler S., Heber U., Napiwotzki R., Hagen H.J. 1995b, *A&A* 303, L53
 Dreizler S., Werner K., Heber U., Engels D. 1996, *A&A* 309, 820
 Dreizler S., Werner K., Heber U., Reid N., Hagen H. 1997, in: *Proceedings of the 3rd Conference on Faint Blue Stars*, eds. A.G.D. Philip, J. Liebert & R.A. Saffer, R.A., L. Davis Press, Schenectady, USA, p. 303
 Driebe T., Schönberner D., Blöcker T., Herwig F. 1998, *A&A* 339, 123
 Drilling J.S., Schönberner D. 1985, *A&A* 146, L23
 Finley D.S., Koester D., Basri G. 1997, *ApJ* 488, 375
 Fontaine G., Wesemael F. 1987, in: *IAU Coll. No. 95, The second conference on faint blue stars*, eds. A.G.D. Philip, D.S. Hayes & J.W. Liebert, L. Davis Press, p. 319
 Fontaine G., Wesemael F. 1997: in: *White dwarfs*, eds. I. Isern, M. Hernanz & E. García-Berro, Kluwer, Dordrecht, p. 173
 Górný S.K., Stasińska G., Tylenda R. 1997, *A&A* 318, 256
 Green R.F., Schmidt M., Liebert J. 1986, *ApJS* 61, 305
 Griem H.R. 1974, *Spectral line broadening by plasmas*, Academic Press, New York & London
 Harrison T.E. 1996, *PASP* 108, 1112
 Heber U., Werner K., Drilling J.S. 1988, *A&A* 194, 223
 Herrero A., Manchado A., Méndez R.H. 1990, *Ap&SS* 169, 183
 Hoare M.G., Drake J.J., Werner K., Dreizler S. 1996, *MNRAS* 283, 830
 Holberg J.B. 1987, in: *IAU Coll. 95, The second conference on faint blue stars*, eds. A.G.D. Phillip, D.S. Hayes & J. Liebert, L. Davis Press, p. 285
 Homeier D., Koester D., Hagen H.-J., et al. 1998, *A&A* 338, 563
 Hubeny I., Hummer D.G., Lanz T. 1994, *A&A* 282, 151
 Hummer D.G., Mihalas D. 1988, *ApJ* 331, 794

Husfeld D. 1987, in: IAU Coll. 95, The second conference on faint blue stars, eds. A.G.D. Philips, D.S. Hayes, J.W. Liebert, L. Davis Press, p. 237

Husfeld D., Butler K., Heber U., Drilling J.S. 1989, *A&A* 222, 150

Iben I.Jr. 1986, *ApJ* 304, 201

Iben I.Jr., Livio M. 1993, *PASP* 105, 1373

Iben I.Jr., Tutukov A.V. 1985, *ApJS* 58, 661

Iben I.Jr., Tutukov A.V. 1986, *ApJ* 311, 742

Iben I.Jr., Tutukov A.V. 1993, *ApJ* 418, 343

Iben I.Jr., Kaler J.B., Truran J.W., Renzini A. 1983, *ApJ* 264, 605

Ishida K., Weinberger R. 1987, *A&A* 178, 227

Jordan S., Heber U., Weidemann V. 1991, in: White dwarfs, eds. G. Vauclair & E.M. Sion, Kluwer, Dordrecht, p. 121

Kippenhahn R., Kohl K., Weigert A. 1967, *Zeitschrift f. Astrophys.* 66, 58

Koester D., Schönberner D. 1986, *A&A* 154, 125

Koesterke L., Hamann W.-R. 1997, *A&A* 320, 91

Kubát J. 1995, *A&A* 299, 803

Kwitter K.B., Jacoby G.H., Lydon T.J. 1988, *AJ* 96, 997

Lemke M., 1997, *A&AS* 122, 285

Leuenhagen U., Hamann W.-R., Jeffery C.S. 1996, *A&A* 312, 167

Liebert J. 1986, in: Hydrogen deficient stars and related objects, eds. K. Hunger, D. Schönberner & N. Kameswara Rao, Reidel Publ., Dordrecht, p. 367

Liebert J., Bergeron P. 1995, in: White dwarfs, eds. D. Koester & K. Werner, Springer-Verlag, Berlin, Heidelberg, p. 12

Liebert J., Green R., Bond H.E., et al. 1989, *ApJ* 346, 251

Liebert J., Bergeron P., Tweedy R.W. 1994, *ApJ* 424, 817

Liebert J., Tweedy R.W., Napiwotzki R., Fulbright M.S. 1995, *ApJ* 441, 424

Livio M. 1993, in: IAU Symp. 155, Planetary nebulae, eds. R. Weinberger & A. Acker, Kluwer Academic Publ., Dordrecht, p. 279

McCarthy J.K. 1988, PhD thesis, CalTech, Pasadena

McCarthy J.K., Méndez R.H., Kudritzki R.P. 1997, IAU Symp. 180, Planetary Nebulae, eds. H.J. Habing & H.J.G.L.M. Lamers, Kluwer, Dordrecht, p. 120

Méndez, R.H. 1991, in: IAU Symp. 145, Evolution of stars: the photospheric abundance connection, eds. G. Michaud & A. Tutukov, Kluwer Academic Publ., Dordrecht, p. 375

Méndez R.H., Kudritzki R.P., Gruschinske J., Simon K.P. 1981, *A&A* 101, 323

Méndez R.H., Kudritzki R.P., Herrero A., Husfeld D., Groth H.G. 1988a, *A&A* 190, 113

Méndez R.H., Groth H.G., Husfeld D., Kudritzki R.P., Herrero A., 1988b, *A&A* 197, L25

Méndez R.H., Kudritzki R.P., Herrero A. 1992, *A&A* 260, 329

Napiwotzki R. 1992, in: The atmospheres of early-type stars, Lecture notes in physics 401, eds. U. Heber & C.S. Jeffery, Springer-Verlag Berlin, Heidelberg, New York, p. 310

Napiwotzki R. 1993a, *Acta Astron.* 43, 343

Napiwotzki R. 1993b, PhD thesis, Universität Kiel

Napiwotzki R. 1995, in: White dwarfs, eds. D. Koester & K. Werner, Springer-Verlag, Berlin, Heidelberg, New York, p. 176

Napiwotzki R. 1997, *A&A* 322, 256

Napiwotzki R. 1998, in: Stars and galaxies, Reviews in modern astronomy 11, Astronomische Gesellschaft, Hamburg, p. 3

Napiwotzki R., Rauch T. 1994, *A&A* 285, 603

Napiwotzki R., Schönberner D. 1991a, *A&A* 249, L16 (Paper II)

Napiwotzki R., Schönberner D. 1991b, in: White dwarfs, eds. G. Vauclair & E. Sion, Kluwer, Dordrecht, p. 39

Napiwotzki R., Schönberner D. 1993, in: in: White dwarfs: advances in observation and theory, ed. M.A. Barstow, Kluwer, Dordrecht, p. 99

Napiwotzki R., Schönberner D. 1995, *A&A* 301, 545 (Paper III)

Napiwotzki R., Hurwitz M., Jordan S., et al. 1995, *A&A* 300, L5

Napiwotzki R., Green P.J., Saffer R.A. 1999, *ApJ* 517, 399

Naylor T., Charles P.A., Mukai K., Evans A. 1992, *MNRAS* 258, 449

Peña M., Ruiz M.T., Bergeron P., Torres-Peimbert S., Heathcote S. 1997, *A&A* 317, 911

Pottasch S.R. 1996, *A&A* 307, 561

Press W.H., Teukolsky S.A., Vetterling W.T., Flannery B.P. 1992, Numerical recipes, Cambridge University Press

Prialnik D., Kovetz A. 1995, *ApJ* 445, 789

Rauch T. 1993, *A&A* 276, 171

Rauch T., Werner K. 1997, in: Proceedings of the 3rd Conference on Faint Blue Stars, eds. A.G.D. Philip, J. Liebert & R.A. Saffer, R.A., L. Davis Press, Schenectady, USA, p. 217

Rauch T., Heber U., Hunger K., Werner K., Neckel T. 1991, *A&A* 241, 457

Rauch T., Dreizler S., Wolff B. 1998, *A&A* 338, 651

Rauch T., Köppen J., Napiwotzki R., Werner K. 1999, *A&A* 347, 169

Reynolds R.J. 1987, *ApJ* 315, 234

Ringwald F.A., Naylor T., Mukai K. 1996, *MNRAS* 281, 192

Saurer W., Werner K., Weinberger R. 1997, *A&A* 328, 598

Schönberner D. 1979, *A&A* 79, 108

Schönberner D. 1981, *A&A* 103, 119

Schönberner D. 1983, *ApJ* 272, 708

Schönberner D., Napiwotzki R. 1990, *A&A* 231, L33 (Paper I)

Schöning T., Butler K. 1989, *A&AS* 78, 51

Shamey L.J. 1964, PhD thesis, B.S. Loyola University of Los Angeles

Shara M.M., Moffat A.F.J., Webbink R.F. 1985, *ApJ* 294, 271

Shara M.M., Prialnik D., Kovetz A. 1993, *ApJ* 406, 220

Slavin A.J., O'Brien T.J., Dunlop J.S. 1995, *MNRAS* 276, 353

Stasińska G., Górný S.K., Tylenda R. 1997, *A&A* 327, 736

Tweedy R.W. 1995, *ApJ* 438, 917

Tweedy R.W., Kwitter K.B. 1994, *AJ* 108, 188

Tweedy R.W., Napiwotzki R. 1994, *AJ* 108, 978

Unglaub K., Bues I. 1998, *A&A* 338, 75

Vassiliadis E., Wood P.R. 1994, *ApJS* 92, 125

Vennes S., Pelletier C., Fontaine G., Wesemael F. 1988, *ApJ* 331, 876

Vennes S., Thejll P.A., Galvan R.G., Dupuis J. 1997, *ApJ* 480, 714

Vidal C.R., Cooper J., Smith E.W. 1970, *JQSRT* 10, 1011

Warner B. 1995, Cataclysmic variable stars, Cambridge University Press

Webbink R.F. 1990, in: Accretion-powered Compact Binaries, ed. C.W. Mauche, Cambridge University Press, p. 177

Werner K. 1986, *A&A* 161, 177

Werner K. 1996, *ApJ* 457, L39

Werner K., Wolff B., Pakull M., et al. 1996, in: Supersoft X-ray sources, ed. J. Greiner, LNP 472, Springer-Verlag, Berlin, p. 131

Werner K., Bagschik K., Rauch T., Napiwotzki R. 1997, A&A 327, 721

Zanin C., Weinberger R. 1997, in: IAU Symp. 180, Planetary Nebulae, eds. H.J. Habing & H.J.G.L.M. Lamers, Kluwer, Dordrecht, p. 290

Appendix A: A compilation of CSPN and white dwarf parameters from literature

Parameter determinations of CSPN and hot white dwarfs and related objects are widely scattered through literature. Many sources are not easily accessible. For this reason we provide a table with parameters and references of the objects displayed in Fig. 2. This compilation may be useful for future investigations. The most obvious application is the selection of candidates for deep imaging to look for faint PNe. We tried to collect all data for central stars and pre-white dwarfs with temperatures higher than 30000 K from literature, which were analyzed with state-of-the-art techniques. Stars already analyzed in this paper (cf. Table 1) are omitted from Table A.2. We used the same lower temperature limit for the white dwarfs, but did not aim for completeness for the cooler DA white dwarfs ($T_{\text{eff}} < 60000$ K). The results are provided in Table A.2. The stars are grouped according to their spectral classes and their temperature. References are given in Table A.1. Objects in globular clusters were excluded from this compilation.

While the DAO and DA analyses are usually based on LTE model atmospheres (with the exception of the Napiwotzki et al. 1999 analysis), NLTE analyses were performed for all other stars listed in Table A.2. Since deviations from LTE produce significant effects in the hottest DA and DAO white dwarfs (Napiwotzki 1997; Napiwotzki et al. 1999), one should be aware of possible systematic effects.

Table A.1. References for Table A.2

- 1 Barstow et al. (1995)
- 2 Bauer & Husfeld (1995)
- 3 Bergeron et al. (1994)
- 4 Dreizler & Heber (1998)
- 5 Dreizler & Werner (1996)
- 6 Dreizler et al. (1995a)
- 7 Dreizler et al. (1995b)
- 8 Dreizler et al. (1997)
- 9 Finley et al. (1997)
- 10 Heber et al. (1988)
- 11 Herrero et al. (1990)
- 12 Hoare et al. (1996)
- 13 Homeier et al. (1998)
- 14 Husfeld D. (1987)
- 15 Husfeld et al. (1989)
- 16 Liebert & Bergeron (1995)
- 17 Liebert et al. (1995)
- 18 McCarthy (1988)
- 19 McCarthy et al. (1997)
- 20 Méndez et al. (1988a)
- 21 Méndez et al. (1992)
- 22 Napiwotzki (1993a)
- 23 Napiwotzki et al. (1995)
- 24 Napiwotzki et al. (1999)
- 25 Peña et al. (1997)
- 26 Rauch (1993)
- 27 Rauch et al. (1991)
- 28 Rauch et al. (1998)
- 29 Rauch & Werner (1997)
- 30 Rauch et al. (1999)
- 31 Reynolds (1987)
- 32 Saurer et al. (1997)
- 33 Tweedy & Kwitter (1994)
- 34 Werner et al. (1996)
- 35 Werner et al. (1997)
- 36 Zanin & Weinberger (1997)

Table A.2. Fundamental parameters of hot CSPN, white dwarfs, and related objects compiled from the literature

Name	T_{eff}	$\log g$	PN	Ref.	Name	T_{eff}	$\log g$	PN	Ref.	Name	T_{eff}	$\log g$	PN	Ref.
O(H) stars					PG 0108+101	95.0	7.50	?	6	PG 1040+451	49.2	7.70	–	9
K 1-22	141.0	6.73	+	30	MCT 2148–294	85.0	7.50	–	8	RE 1711+664	49.0	8.89	–	24
BDz 1	128.0	6.85	+	30	PG 0046+078	73.0	8.00	–	6,31	GD 8	48.7	7.74	–	9
A 20	119.0	6.13	+	30	PG 0237+116	70.0	8.00	–	6	RE 0427+740	48.6	7.93	–	24
NGC 2438	114.0	6.62	+	30	RE 0503–289	70.0	7.50	–	6	MCT 2153–4156	48.2	7.98	–	9
NGC 1360	110.0	5.60	+	12	HS 0111+0012	65.0	7.80	–	6	RE 1529+483	47.7	7.65	–	9
A 15	110.0	5.70	+	19	Lanning 14	58.0	7.90	–	6	PG 1526+013	47.3	7.81	–	9
BE UMa	105.0	6.50	+	17	PG 0929+270	55.0	7.90	–	8	RE 2004–560	47.2	7.63	–	9
LSS 1362	100.0	5.30	+	10	HZ 21	53.0	7.80	–	6	PG 1642+386	47.1	7.55	–	9
NGC 2022	100.0	5.30	+	19	PG 1057–059	50.0	7.90	–	8	RE 0003+433	46.7	8.88	–	9
MeWe 1-3	100.0	5.50	+	32	HD 14949B	49.5	7.97	–	23	PG 1232+238	46.6	7.83	–	24
IC 289	100.0	5.60	+	19	HS 0103+2947	49.5	8.00	–	6	GD 2	46.5	7.83	–	24
NGC 2610	100.0	5.80	+	19	PG 1133+489	46.0	8.00	–	8	RE 1746–703	46.4	8.97	–	9
HaTr 7	100.0	6.00	+	32	DAO white dwarfs					GD 257	46.0	7.67	–	9
EGB 6	100.0	7.00	+	16	Wray 17-31	69.2	7.14	+	25	PG 1010+064	45.6	7.77	–	9
A 36	95.0	5.30	+	18	Ton 320	68.8	7.68	?	3,33	PG 0916+065	45.4	7.73	–	3
DHW 1-2	90.0	5.00	+	32	HS 2115+1148	67.0	6.90	–	7	KUV 343-6	45.4	7.39	–	9
Lo 8	90.0	5.10	+	11	Ton 353	66.1	7.11	–	3	RE 1546–364	45.2	8.88	–	9
LSS 2018	90.0	5.10	+	11	LB 2	65.7	7.67	–	3	RE 2324–544	45.0	7.94	–	9
J 320	85.0	4.70	+	19	PG 0834+501	60.4	7.11	–	3	GD 984	44.9	7.77	–	24
LSE 125	85.0	5.10	+	20	Feige 55	56.7	7.06	–	3	RE 1800+683	44.7	7.80	–	24
NGC 7009	82.0	4.90	+	21	PG 0134+181	56.4	7.40	–	3	RE 2156–543	44.3	7.91	–	9
NGC 4361	82.0	5.50	+	21	RE 1016–053	56.4	7.74	–	3	RE 0632–050	44.1	8.39	–	9
BD+28°4211	82.0	6.20	?	22,36	RE 0720–318	53.6	7.64	–	1	RE 1820+580	44.1	7.78	–	24
NGC 3242	75.0	4.75	+	21	PG 1413+015	48.1	7.69	–	3	RE 0715–702	43.9	8.05	–	9
KS 292	75.0	5.00	–	27	PG 2013+400	47.8	7.69	–	3	RE 1032+532	43.6	7.95	–	24
Feige 67	75.0	5.20	–	2	PG 1210+533	44.8	7.89	–	3	PG 2303+017	43.3	7.85	–	9
NGC 1535	70.0	4.65	+	21	PG 1305–017	44.4	7.76	–	3	PG 1648+371	42.0	7.83	–	9
IC 2448	65.0	4.80	+	21	DA white dwarfs					HS 1950–432	41.3	7.85	–	9
NGC 6058	65.0	4.80	+	11	PG 0948+534	126.3	7.27	–	16	RE 1043+490	41.1	7.94	–	24
Vy 1-1	60.0	4.20	+	19	HS 2246+0640	98.0	7.04	–	13	PG 1057+719	41.1	7.84	–	24
NGC 6210	50.0	3.90	+	18	HS 0615+6535	98.0	7.07	–	13	RE 1629+780	41.0	7.92	–	24
NGC 6891	50.0	4.00	+	21	RE 1738+665	95.3	7.86	?	9,33	PG 2150+021	40.6	7.76	–	9
NGC 6826	50.0	4.00	+	21	PG 1342+444	78.7	7.82	–	3	PG 0136+251	40.3	8.93	–	9
IC 4637	50.0	4.05	+	21	PG 1622+323	77.2	7.84	–	9	Ton 61	39.8	7.78	–	24
IC 3568	50.0	4.05	+	21	HS 1749+7145	76.9	7.56	–	13	GD 394	39.6	7.94	–	9
NGC 2392	47.0	3.80	+	21	HS 1827+7753	75.8	7.68	–	13	GD 50	39.5	9.07	–	24
NGC 6629	47.0	3.90	+	21	RE 0633+200	75.8	8.40	–	9	GD 153	38.9	7.78	–	24
EGB 5	42.0	5.80	+	20	PG 1547+015	73.0	7.63	–	9	RE 0841+032	38.3	7.75	–	24
HD 128220	40.6	4.50	–	26	RE 0443–034	72.3	8.77	–	9	RE 1650+403	38.1	7.97	–	24
IC 4593	40.0	3.60	+	21	HS 2244+0305	72.0	7.78	–	13	PG 2349+286	38.1	7.78	–	9
DdDm 1	37.0	3.40	+	19	Ton 60	69.7	7.01	–	9	RE 1446+632	37.9	7.79	–	24
IC 418	36.0	3.45	+	21	Ton 21	69.7	7.47	–	9	PG 1603+432	36.3	7.85	–	9
He 2-182	36.0	3.50	+	21	PG 1532+033	69.5	7.76	–	9	RE 1440+750	36.2	8.87	–	24
He 2-108	33.0	3.30	+	21	MCT 2146–4320	67.9	7.58	–	9	RE 1845+682	36.1	8.23	–	24
Tc 1	33.0	3.30	+	21	LB 1628	66.4	7.75	–	9	PG 0937+506	36.0	7.69	–	24
M 1-26	33.0	3.30	+	21	RE 2214–491	66.1	7.38	–	9	RE 0723–274	35.9	7.84	–	9
H 2-1	33.0	3.35	+	21	PG 1141+078	66.0	7.57	–	3	GD 659	35.8	7.68	–	9
O(He) stars					KUV 343–7	65.8	7.67	–	9	RE 1024–302	35.7	8.95	–	9
HS 1522+6615	140.0	5.50	–	28	HS 0951+3620	65.0	7.66	–	13	PG 1026+454	35.5	7.70	–	24
LoTr 4	120.0	5.50	+	28	RE 0029–632	63.7	7.96	–	9	PG 1636+351	35.4	7.98	–	24
K 1-27	105.0	6.50	+	28	KPD 2046+3940	63.2	7.77	–	9	RE 0605–482	35.3	7.84	–	9
HS 2209+8229	100.0	6.00	–	28	Feige 24	62.7	7.17	–	9	KPD 0416+4015	35.2	7.75	–	9
LSE 259	75.0	4.40	–	15	PG 2244+031	62.3	7.72	–	9	Feige 31	35.1	7.64	–	9
LSE 153	70.0	4.75	–	15	PG 2353+026	62.0	7.74	–	9	GD 336	34.4	7.91	–	24
LSE 263	70.0	4.90	–	15	G 191 B2B	61.2	7.49	–	9	PG 2120+054	34.2	7.80	–	9
BD+37°442	60.0	4.00	–	14	HS 0742+2306	60.0	7.66	–	13	RE 1943+500	34.1	7.97	–	9
PG 1159 stars					RE 0558–373	59.6	7.44	–	9	Feige 93	34.0	7.43	–	9
RXJ 0122.9–7521	180.0	7.50	–	34	RE 0623–374	58.2	7.27	–	9	RE 0239+500	33.8	8.47	–	9
H 1504+65	170.0	8.00	–	6	MCT 2159–4129	56.4	7.84	–	9	GD 80	33.5	8.01	–	9
RXJ 2117.1+3412	170.0	6.00	+	29	PG 1234+481	56.4	7.67	–	9	LB 1663	33.4	7.85	–	9
NGC 246	150.0	5.70	+	29	PG 1548+405	56.2	7.75	–	9	RE 0521–102	33.2	8.60	–	24
PG 1144+005	150.0	6.50	–	6	PG 2331–4731	55.8	8.07	–	9	KPD 1914+0929	33.1	7.79	–	9
PG 1520+525	150.0	7.50	+	4	RE 2024+200	55.8	7.75	–	9	Ton 210	32.9	7.92	–	9
PG 1159–035	140.0	7.00	–	4	RE 0720–314	55.1	7.92	–	9	GD 71	32.7	7.68	–	9
HS 2324+3944	130.0	6.20	–	6	PG 0836+237	54.6	7.60	–	9	Ton S 72	32.5	8.09	–	9
Lo 4	120.0	5.50	+	6	PG 1123+189	54.3	7.76	–	24	PG 0904+511	32.2	8.11	–	24
PG 1424+535	110.0	7.00	–	4	LB 335	53.6	8.23	–	24	PHL 1400	32.1	8.45	–	24
HS 1517+7403	110.0	7.00	–	4	GD 246	53.1	7.85	–	24	RE 0512–004	31.7	7.40	–	24
PG 2131+066	95.0	7.50	–	4	PG 1657+343	53.0	7.76	–	9	RE 1019–140	31.5	7.92	–	24
MCT 0130–1937	90.0	7.50	–	4	RE 0620+132	52.9	7.83	–	9	RE 1847–221	31.5	8.17	–	9
PG 1707+427	85.0	7.50	–	4	RE 0957+852	51.3	8.37	–	24	GD 38	31.3	7.87	–	9
PG 0122+200	80.0	7.50	–	6	RE 0457–280	51.2	7.72	–	24	PG 1609+631	31.0	8.41	–	9
HS 0704+6153	75.0	7.00	–	4	HZ 43	50.8	7.99	–	9	RE 0809–725	30.6	7.90	–	9
DO white dwarfs					RE 2116+735	50.8	7.72	–	24	PG 1125–026	30.7	8.24	–	24
KPD 0005+5106	120.0	7.00	–	6	RE 0550–240	50.7	8.07	–	9	PG 1041+580	30.3	7.81	–	24
PG 0038+199	115.0	7.50	–	6	PG 0824+288	50.5	7.43	–	9	GD 421	30.2	7.63	–	9
PG 0109+111	110.0	8.00	?	6,35	PG 2357+296	49.9	7.60	–	9	RE 0831–534	30.2	8.01	–	9
PG 1034+001	100.0	7.50	–	6	RE 2127–221	49.8	7.65	–	9	PG 1620+647	30.2	7.72	–	9
HS 1830+7209	100.0	7.20	–	6	PG 1403–077	49.3	7.59	–	9					

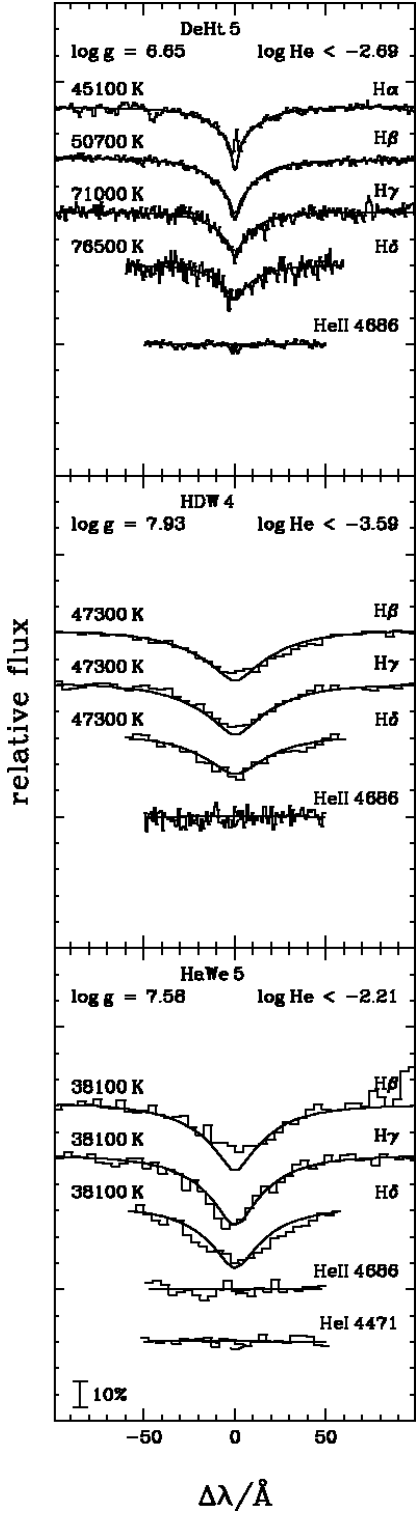


Fig. 9. DA central stars. The synthetic spectra of the helium lines are computed for the 3σ limit of the helium abundance

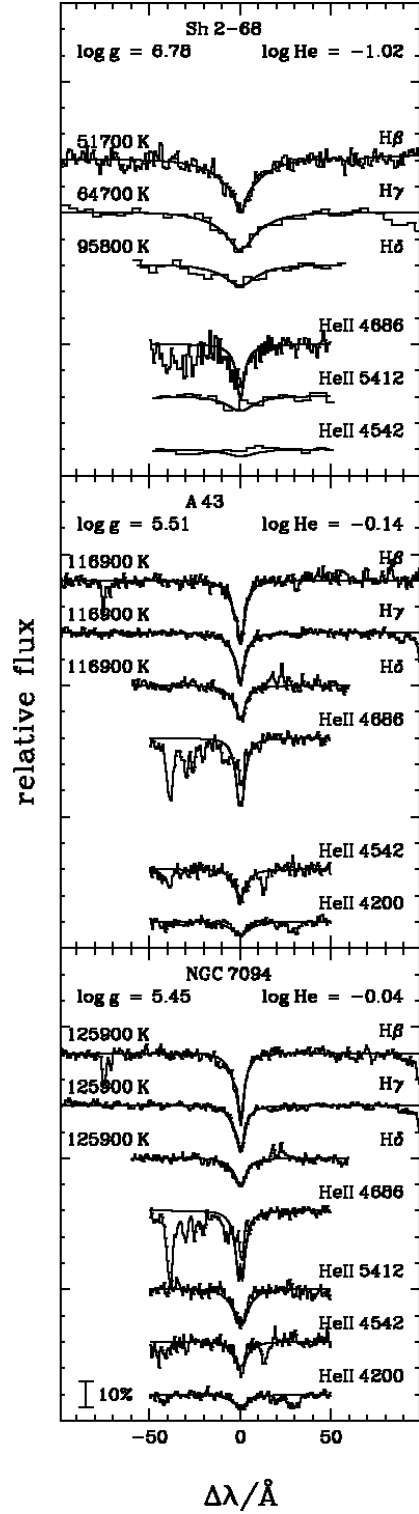


Fig. 10. Fits of the hybrid PG 1159 stars. The He II 4686 Å lines of A 43 and NGC 7094 were not used for the fit. The observed and theoretical spectra are only shown for comparison purposes

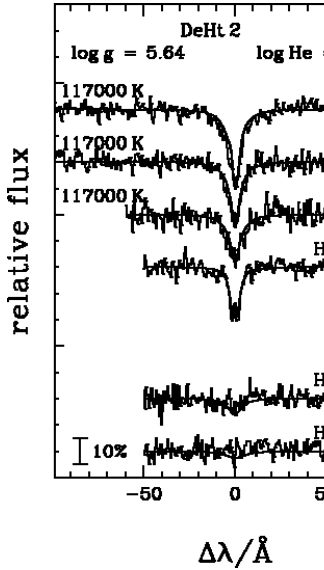


Fig. 11. Fit of the high luminosity central star DeHt 2

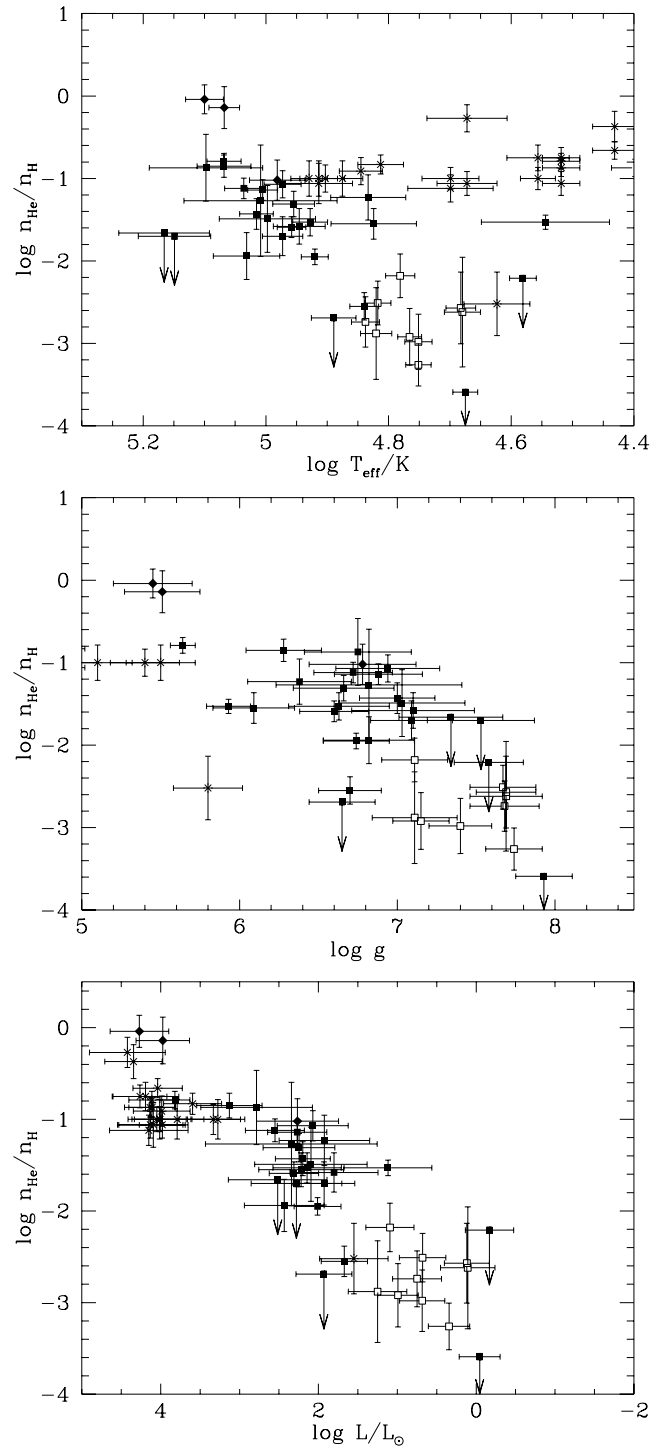


Fig. 12. Photospheric helium abundance as function of effective temperature, gravity, and luminosity (top to bottom). Our results (filled squares; hybrid CSPN: filled diamonds) are supplemented with the DAO white dwarfs analysed by Bergeron et al. (1994; open squares) and the CSPN analysis of Méndez et al. (1988a; stars). Upper limits are marked by arrows